Physics – Uspekhi **42** (1) 7 – 36 (1999)

REVIEWS OF TOPICAL PROBLEMS PACS numbers: 02.50.Ey, **05.40.+j**, **05.45.+b**, **87.70.+c**

Stochastic resonance: noise-enhanced order

V S Anishchenko, A B Neiman, F Moss, L Schimansky-Geier

Contents

Abstract. Stochastic resonance (SR) provides a glaring example of a noise-induced transition in a nonlinear system driven by an information signal and noise simultaneously. In the regime of SR some characteristics of the information signal (amplification factor, signal-to-noise ratio, the degrees of coherence and of order, etc.) at the output of the system are significantly improved at a certain optimal noise level. SR is realized only in nonlinear systems for which a noise-intensity-controlled characteristic time becomes available. In the present review the physical mechanism and methods of theoretical description of SR are briefly discussed. SR features determined by the structure of the information signal, noise statistics and properties of particular systems with SR are studied. A nontrivial phenomenon of stochastic synchronization defined as locking of the instantaneous phase and switching frequency of a bistable system by external periodic force is analyzed in detail. Stochastic synchronization is explored in single and coupled bistable oscillators, including ensembles. The effects of SR and stochastic synchronization of ensembles of stochastic resonators are studied both with and without coupling between the elements. SR is considered in dynamical and nondynamical (threshold) systems. The SR effect is analyzed from the viewpoint of information and entropy characteristics of the signal, which determine the degree of order or self-organization in the system. Applications of the SR concept to explaining the results of a series of biological experiments are discussed.

V S Anishchenko N G Chernyshevskiĭ Saratov State University, Department of Physics
ul. Astrakhanskaya 83, 410026 Saratov, Russia
Tel./Fax (7-8452) 51-45 49
E-mail: wadim@chaos.ssu.runnet.ru
A B Neiman N G Chernyshevskiĭ Saratov State University, Department of Physics
ul. Astrakhanskaya 83, 410026 Saratov, Russia
University of Missouri at St. Louis, Department of Physics and Astronomy, St. Louis, MO 63121 USA
F Moss University of Missouri at St. Louis, Department of Physics and Astronomy, St. Louis, MO 63121 USA
Tel. (1-314) 516-6150. Fax (1-314) 516-6152
E-mail: mossf@umslvma.umsl.edu
L Schimansky-Geier Humboldt University at Berlin
Invalidenstr. 110, D-10115 Berlin, Germany
Tel. (49-30) 2093-7624. Fax (49-30) 2093-7638
E-mail: alsg@summa.physik.hu-berlin.de

Received 26 June 1998, revised 6 August 1998
Uspekhi Fizicheskikh Nauk **169** (1) 7 – 38 (1999)
Translated by the authors; edited by A Radzig

1. Introduction

The word 'noise' in ordinary consciousness is associated with the term 'hindrance'. It was traditionally considered that the presence of noise can only make the operation of any system

worse. There are well-known classical radiophysical problems related to limitations of the sensitivity of amplifiers and to a finiteness of the pulse bandwidth of oscillators due to the presence of natural and technical noise [1 – 3]. Fluctuation phenomena are typical for all real systems because of the discrete structure of matter and cannot be eliminated in principal. Since L Boltzmann, the limitation of the purely deterministic description of evolutionary processes has become clear, which accelerated the development of statistical physics. Founders of the theory of nonlinear oscillations also realized this limitation. Already in 1933 they raised the question of a statistical consideration of dynamical systems, serving as a background for further studies in the field of statistical radiophysics [4].

Recently it has been established that the presence of noise sources in nonlinear dynamical systems can induce completely new regimes that cannot be realized without noise, for example, noise-induced self-sustained oscillations [5]. These effects were called noise-induced transitions [6]. The variety and complexity of the transitions in nonlinear dynamical systems produced the following questions, quite surprising until recently: does noise always disorder a system's behaviour, or are there cases when noise enhances the degree of order in a system or evokes improvement of its performance? Recent studies have convincingly shown that in nonlinear systems noise can induce new, more ordered, regimes, lead to the formation of more regular structures or increase the degree of coherence, cause the amplification of weak signals and growth of their signal-to-noise ratio. In other words, noise can play a constructive role, enhancing the degree of order in a system.

Stochastic resonance (SR) is one of the most shining and relatively simple examples of this type of nontrivial behaviour of nonlinear systems under the influence of noise. The notion of SR determines a group of phenomena wherein the response of a nonlinear system to a weak input signal can be significantly increased with appropriate tuning of the noise intensity. At the same time, the integral characteristics of the process at the output of the system, such as the spectral power amplification (SPA), the signal-to-noise ratio (SNR) or input/output cross-correlation measures have a well-marked maximum at a certain optimal noise level. Besides, an entropy-based measure of disorder attains a minimum, showing the increase of noise-induced order.

The term 'stochastic resonance' was introduced by Benzi, Sutera and Vulpiani [7 – 9] in 1981 – 1982, when they were exploring a model of a bistable oscillator proposed for explanation of the periodic recurrences of the Earth's ice ages. The model described the motion of a particle subject to large friction in a symmetric double-well potential, driven by a periodic force. Two stable states of the system represented the ice period and the optimal normal climate of the Earth. The periodic force referred to the oscillations of the eccentricity of the Earth's orbit. Estimations have shown that the actual amplitude of the periodic force is far too small to cause the system to switch from one state to another one. The possibility of switchings was achieved with the introduction of additional random force which induced transitions from one potential well to another over the potential barrier of the system.

In 1983, SR was studied experimentally in the Schmitt trigger system where the SNR was first used to describe the phenomenon [10]. In has been shown that the SNR at the output of the Schmitt trigger subjected to a weak periodic signal and noise increases with increasing noise intensity, passes through a maximum and then decreases. By this means there is an optimal noise level at which the periodic component of the signal is maximized.

Thereafter the effect of SR has been found and studied in a variety of physical systems, namely, in a ring laser [11], in magnetic systems [12], in passive optical bistable systems [13], in systems with electronic paramagnetic resonance [14], in experiments with Brownian particles [15], in experiments with magnetoelastic ribbons [16], in a tunnel diode [17], in superconducting quantum interference devices (SQUIDs) [18], and in ferromagnetics and ferroelectrics [19 – 21]. SR has equally been observed in chemical systems [22 – 24] and even in social models [25].

It was shown that SR refers to a generic physical phenomenon typical for nonlinear systems in which one of the characteristic time scales is controlled by noise. The physical mechanism of SR is rather simple and can be illustrated using an overdamped bistable system.

SR: physical background. Let us consider qualitatively the motion of a Brownian particle in a system with a symmetric double-well potential $U(x) = -0.5x^2 + 0.25x^4$ subjected to a weak periodic force $A \sin \omega t$. In the absence of periodic modulation ($A = 0$), the system possesses two characteristic time scales. The first is defined by random walks of the particle in the vicinity of one of the equilibrium positions (the intrawell or local dynamics). The second time scale characterizes the mean time of barrier crossing and refers to the global dynamics of noise-induced transitions between the potential wells. Note that the amplitude of the periodic force A is assumed to be small in the sense that switchings between the potential wells are excluded in the absence of noise. In the frequency region the second time scale corresponds to the mean rate (or frequency) of escape from a metastable state, known as the Kramers rate [26, 27].

In the case of white noise, parabolic potential wells and a relatively high potential barrier, the Kramers rate is described by the Arrhenius law:

$$r_{\mathrm{K}} = \frac{1}{2\pi} \left[|U''(0)| U''(c) \right]^{1/2} \exp\left(-\frac{\Delta U_0}{D} \right),$$

where $U'' = \mathrm{d}^2 U(x)/\mathrm{d}x^2$, c is the coordinate of the potential minimum, ΔU_0 is the barrier height, and D is the noise intensity. The Kramers rate also determines the probabilities of switching events.

In the presence of a periodic force the potential wells oscillate periodically (Fig. 1). The probabilities of switching events also become the periodic functions of time, and the output signal contains a periodic component.

Figure 2 presents a time series at the output of a bistable system with regard to the intrawell dynamics (a), a similar time series showing only the barrier crossing events (two-state filtering) (b), and the power spectrum (c) of the time series in (b).

The periodic modulation of the potential leads to a periodic modulation of both the barrier height $\Delta U \simeq \Delta U_0 + A \sin \omega t$ and the probability of a switching event. As a result, the power spectrum of the output signal shows a delta-peak at the modulation frequency and at its odd harmonics (in the case of a symmetric potential). Assume that the barrier height ΔU_0, the modulation amplitude and frequency are fixed. The Kramers rate r_{K} will depend only on the noise intensity D. When the noise intensity is small, the

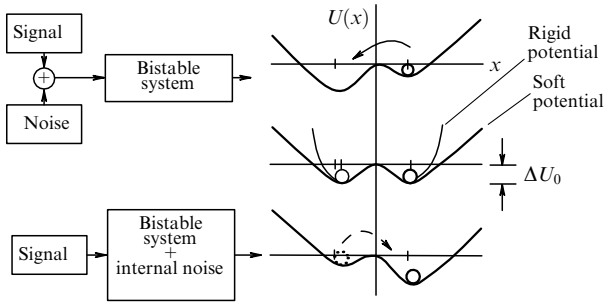

Figure 1. Bistable potential with a weak periodic modulation. The shape of the potential can vary, for example, as shown by the 'rigid' and 'soft' curves. The particle symbolized by the ball can overcome the potential barrier ΔU_0 only in the presence of external or internal noise.

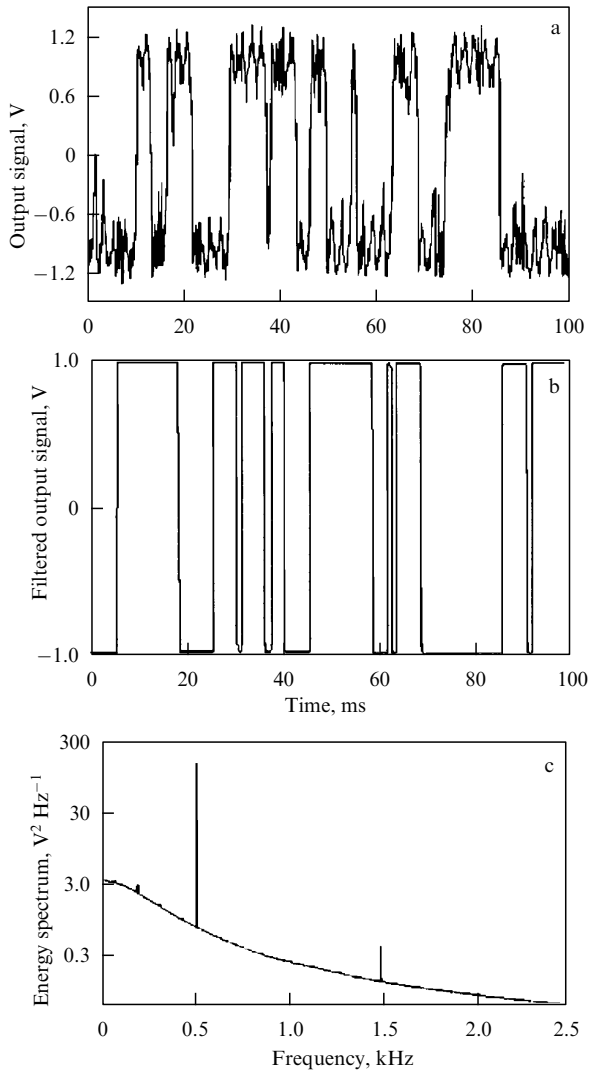

Figure 2. (a) Time series at the output of a bistable system; (b) a similar time series which has been 'two-state filtered'; (c) the power spectrum of the filtered signal.

mean crossing time is too large and considerably exceeds the modulation signal period. When the noise level is high, there is a nonzero probability that the system repeatedly switches within one signal period. By varying the noise intensity, one can ensure a regime when the mean barrier crossing time is close to the modulation signal period. Switching events will occur on average in phase with the external periodic force. Hence by varying the noise intensity, we can tune the stochastic bistable system to a regime of maximal amplification of the modulation signal and the maximal signal-to-noise ratio. This has been confirmed theoretically and experimentally.

Characteristics of SR. An explanation of the physical mechanism of the phenomenon proper and the definition of SR depend in many respects on which quantitative characteristics of SR are calculated analytically and numerically or measured in physical experiments. In the present work we use the spectral power amplification (SPA) η, the signal-to-noise ratio (SNR) and the residence-time distribution density $p(\tau)$ of a particle in one of the potential wells as the main characteristics of SR. In experiments the signal energy is determined as an integral of the power spectral density over the range of measured frequencies [28].

The signal-to-noise ratio is defined as the ratio between the spectral power densities of a signal and noise at the signal frequency. In this work we use a definition of the SNR accepted in radiotechnics as the ratio of the signal energy to the noise energy P_S/P_N. In the case of a harmonic signal at the system input, the SNR can be determined experimentally as the ratio of the height of the modulation signal spectral line over the noise pedestal to the noise background level of the power spectrum of the output signal.

As a result of random switchings, the output of a stochastic bistable system without considering the intrawell dynamics can be represented by a stochastic telegraph signal (see Fig. 2b). The residence time for one of the potential wells is a random quantity whose probability density $p(\tau)$ in the absence of modulation shows evidence of an exponentially decreasing function [29]. When a modulation signal is added, the probability density becomes structured and contains a series of Gaussian-like peaks centred at $\tau = nT_s/2$, $n = 1, 3, 5, \ldots$, where T_s is the modulation signal period. The maxima of $p(\tau)$ decay exponentially with n. In the regime of SR the peak of $p(\tau)$ at $\tau = T_s/2$ is the largest: the switchings between the potential wells are in phase with the external periodic signal and the mean residence time $\langle\tau\rangle$ is most close to half the signal period. The description of SR based on the residence-time distributions, therefore, reflects a synchronization of system switchings by an external periodic force [30, 31].

Since the statistical properties of a telegraph signal depend on the noise intensity, the probability density structure can be controlled by noise variation. In this connection we have an alternative approach to analyzing the mechanisms of SR, based on the studies of residence-time statistics. Of course, the physical mechanism of SR does not depend on how it is described.

As has been noted, SR can be realized in stochastic systems with a noise-controlled characteristic time scale. It is absolutely clear that both the qualitative and quantitative characteristics of SR are largely defined by the properties of particular nonlinear systems. SR can be realized in bistable [7, 32] and monostable [33] dynamical systems as well as in the oscillators of periodic and chaotic signals [34, 35]. SR can also be observed in nondynamical or so-called threshold systems [36, 37]. Characteristics and properties of SR must undoubtedly depend on the structure of signals applied to a nonlinear system. This concerns in equal degree both informational and noisy signals. The modulation signal can be harmonic or

multifrequency or be a narrow-band stochastic process [38]. The stochastic force can be closed to white noise but can also have a finite correlation time and a bounded spectrum [39, 40]. Depending on the signal properties, noise and the particular properties of nonlinear systems, SR is characterized by specific features. At the same time without regard to the system characteristics and the structure of signals SR is determined by its generic property of increasing the degree of order in the output signal for the optimal level of noise. The intention in this review is to stir up a consistent and, where possible, brief discussion of all the above-mentioned aspects of SR phenomenon.

Although it is only about 20 years since the effect of SR was first observed, the number of publications on this problem is huge and still growing. It is very difficult in the frame of one review to cover all the currently available results on SR. The more so as there is no need for this. Four excellent reviews [41 – 44] on SR have been published and two special international conferences were held, whose proceedings were published [45, 46]. A comprehensive database containing more than 300 publications on SR has been installed on the Internet [47].

The authors of this review set themselves a rather modest task of describing those results which have not been reflected in the published reviews or have been covered there very laconically. In this review we present the main results which have been obtained together with our disciples and colleagues during the last five years. We believe that the present review together with those already published will allow our readers to make the most complete view and will help them deeply understand this surprising phenomenon.

2. Response to a weak signal. Theoretical approaches

A theoretical description of SR meets a series of principal difficulties. Even without external harmonic signal it is impossible in the general case to find an exact solution of the Fokker – Planck equation for a time-dependent probability density. For this reason we cannot calculate exactly the correlation functions and power spectral densities. On the other hand, with the periodic force taken into account, certain additional difficulties arise due to the inhomogeneity of the corresponding stochastic process in time.

Consider the model of an overdamped bistable oscillator having become canonic for studying SR. The equation of motion in dimensionless variables reads as

$$\dot{x} = x - x^3 + A\cos(\Omega t + \phi) + \sqrt{2D}\,\xi(t) \tag{2.1}$$

and describes the motion of a Brownian particle (in the limit of high friction) in a double-well potential $U_0(x) = -x^2/2 + x^4/4$, driven by white noise $\xi(t)$ with the intensity D and periodic force $f(t) = A\cos(\Omega t + \phi)$. The corresponding Fokker – Planck equation (FPE) for the probability density $p(x, t; \phi)$ is as follows

$$\frac{\partial p}{\partial t} = -\frac{\partial}{\partial x}\left\{\left[x - x^3 + A\cos(\Omega t + \phi)\right]p\right\} + D\,\frac{\partial^2 p}{\partial x^2}\,. \tag{2.2}$$

This equation can be also written in the operator form

$$\frac{\partial p}{\partial t} = \left[\mathcal{L}_0 + \mathcal{L}_{\rm ext}(t)\right] p\,, \tag{2.3}$$

where

$$\mathcal{L}_0 = -\frac{\partial}{\partial x}(x - x^3) + D\,\frac{\partial^2}{\partial x^2}$$

is the unperturbed Fokker – Planck operator ($A = 0$) and $\mathcal{L}_{\rm ext}(t) = -A\cos(\Omega t + \phi)\,\partial/\partial x$ refers to the periodic perturbation.

Difficulties of the first group are not connected directly with SR and have been discussed in detail in the theory of stochastic processes (see, for instance, Refs [1, 6, 48]). The rapid progress of SR studies has required the establishment of a common theory of stochastic diffusion processes with periodically varying coefficients of drift and diffusion. Such a theory was proposed in Refs [49 – 51] and is an extension of the Floquet theory to the case of FPE with periodic coefficients. One of the main conclusions of the general theory of periodically driven Brownian motion is the result for the asymptotic mean $\langle x(t)\rangle$ or the response

$$\langle x(t)\rangle = \sum_{n=-\infty}^{\infty} M_n \exp\left[{\rm i}n(\Omega_t + \phi)\right], \tag{2.4}$$

where the complex amplitudes M_n depend on the noise intensity D, signal frequency Ω and amplitude A. The SPA η at the fundamental frequency Ω is defined as [50]:

$$\eta = \left(\frac{2|M_1|}{A}\right)^2. \tag{2.5}$$

Difficulties related to the periodic nonstationarity can be formally resolved by extending the system phase space using an additional variable which determines the signal phase evolution: $\dot{\theta} = \Omega$. In order to calculate the spectral power densities we average the results over the initial phase ϕ which is supposed to be a uniformly distributed random quantity [2].

Analytical expressions for the spectral power amplification and the signal-to-noise ratio can be derived via some approximations. One of the main is a weak signal approximation when the response can be considered as linear. Other approximations impose some restrictions on the signal frequency. Further we shall study two approximate theories of SR, namely, the two-state theory proposed in Ref. [28] and the linear response theory [52 – 54] having been applied to SR in Refs [50, 55 – 57].

2.1 Two-state theory of SR

Let us examine a symmetric bistable system with a discrete state variable $x(t) = \pm x_m$. Let $n_\pm(t)$ be the probabilities of residing the system in the corresponding state, satisfying the normalization conditions $n_\pm(t) + n_\mp(t) = 1$. Introducing the probability densities of switchings from one state to another $W_\pm(t)$ we arrive at the master equation

$$\dot{n}_\pm = -\left[W_\pm(t) + W_\mp(t)\right] n_\pm + W_\pm(t)\,. \tag{2.6}$$

This linear equation can be solved analytically for a given $W_\pm(t)$. In Ref. [28], the following form was suggested for the probability densities of switching:

$$W_\pm(t) = r_{\rm K}\exp\left(\pm\frac{Ax_m}{D}\cos\Omega t\right). \tag{2.7}$$

Without external force ($A = 0$), the probability densities of switching coincide with the Kramers rate $r_{\rm K}$ and are

independent of time. For the model (2.1) the Kramers rate is described by the following law if $D < \Delta U = 1/4$:

$$r_{\mathrm{K}} = \frac{1}{\sqrt{2}\,\pi} \exp\left(-\frac{1}{4D}\right). \tag{2.8}$$

Here and further the Kramers rate is written in reduced (dimensionless) quantities.

The master equation (2.6) adequately describes the dynamics of the bistable overdamped oscillator when the signal changes slowly enough so that relaxation processes in the system go much more faster than the external force changes. The equations for conditional probabilities $n_{\pm}(t|x_0, t_0)$, which we need to calculate the autocorrelation function, have the same form as (2.6). A solution of the linear equation (2.6) can be obtained without any difficulty for the case of a weak signal, i.e. $Ax_m \ll D$. In this case one can expand the switching rate in a Taylor power series and retain the linear terms in the signal amplitude only. As a result, the expression for the conditional probability reads as

$$\begin{aligned} n_{+}(t|x_0, t_0) = \frac{1}{2}\Bigg\{ & \exp\left[-2r_{\mathrm{K}}(t - t_0)\right] \\ & \times \left[2\delta_{x_0, x_m} - 1 - \frac{2r_{\mathrm{K}} A x_m \cos(\Omega t_0 + \psi)}{D(4r_{\mathrm{K}}^2 + \Omega^2)^{1/2}}\right] \\ & + 1 + \frac{2r_{\mathrm{K}} A x_m \cos(\Omega t + \psi)}{D(4r_{\mathrm{K}}^2 + \Omega^2)^{1/2}}\Bigg\}, \end{aligned} \tag{2.9}$$

where $\psi = -\arctan(\Omega/2r_{\mathrm{K}})$. Knowledge of the conditional probabilities allows us to calculate any statistical characteristics of the process. The mean value characterizing the system's response and the spectral density that is necessary for estimating the SNR are of great interest. The conditional probability density is determined as $p(x, t|x_0, t_0) = n_{+}(t)\,\delta(x - x_m) + n_{-}(t)\,\delta(x + x_m)$. The mean value is $\langle x(t)|x_0, t_0\rangle = \int x p(x, t|x_0, t_0)\,\mathrm{d}x$. We are interested in the asymptotic limit $\langle x(t)\rangle = \lim_{t_0 \to -\infty} \langle x(t)|x_0, t_0\rangle$, for which from (2.9) we obtain

$$\langle x(t)\rangle = A_1(D)\cos\left[\Omega t + \psi(D)\right], \tag{2.10}$$

where the amplitude $A_1(D)$ and the phase shift $\psi(D)$ are given by the following expressions

$$A_1(D) = \frac{Ax_0^2}{D} \frac{2r_{\mathrm{K}}}{(4r_{\mathrm{K}}^2 + \Omega^2)^{1/2}}, \tag{2.11}$$

$$\psi(D) = -\arctan\frac{\Omega}{2r_{\mathrm{K}}}. \tag{2.12}$$

Knowing the signal amplitude at the output we can determine the SPA as

$$\eta = \frac{4r_{\mathrm{K}}^2 x_m^4}{D^2(4r_{\mathrm{K}}^2 + \Omega^2)}. \tag{2.13}$$

From (2.8) and (2.13) it follows that the SPA attains a single maximum as a function of noise intensity D.

Similarly we can find the autocorrelation function

$$\langle x(t+\tau)x(t)|x_0, t_0\rangle = \iint xyp(x, t+\tau|y, t)p(y, t|x_0, t_0)\,\mathrm{d}x\,\mathrm{d}y$$

and its asymptotic limit for $t_0 \to -\infty$. However, by virtue of periodic modulation the autocorrelation function depends not only on the time shift τ but also periodically on the time t. In order to calculate the spectral density one needs to perform additional averaging over the period of the external force. Such a procedure is equivalent to averaging over an ensemble of the initial random phases and corresponds to experimental methods for measuring the spectral densities and the correlation functions. The expression for the spectral density $G(\omega)$ has the form

$$G(\omega) = G_{\mathrm{N}}(\omega) + \frac{\pi}{2} A_1^2(D)\left[\delta(\omega - \Omega) + \delta(\omega + \Omega)\right] \tag{2.14}$$

and contains two components, namely, a periodic one represented by a delta-function with an appropriate weight, and a noisy component $G_{\mathrm{N}}(\omega)$:

$$G_{\mathrm{N}}(\omega) = \frac{4r_{\mathrm{K}} x_m^2}{4r_{\mathrm{K}}^2 + \omega^2}\left[1 - \frac{A_1^2(D)}{2x_m^2}\right]. \tag{2.15}$$

As seen from the last expression, the noise background is represented by the sum of the unperturbed spectrum (for $A = 0$) $G_{\mathrm{N}}^{(0)}(\omega) = 4r_{\mathrm{K}} x_m^2/(4r_{\mathrm{K}}^2 + \omega^2)$ and a certain additional term of order A^2: $G_{\mathrm{N}}(\omega) = G_{\mathrm{N}}^{(0)}(\omega) + \mathcal{O}(A^2)$. The spectral density of the unperturbed system is determined by the noise intensity D that is involved in the expression for the Kramers rate r_{K} (2.8). The explicit expression for the unperturbed spectral density is given by formula (2.25). For small D, the Kramers rate is small and the spectrum is centred in the low-frequency range. With increasing noise intensity the Kramers rate rises exponentially and the spectrum becomes more uniform. The appearance of the additional term reducing the noise background is explained by the fact that for the two-state model the energy of the output process constitutes $2\pi x_M^2$ and does not depend on the signal amplitude and frequency.

The signal-to-noise ratio for the two-state model reads as

$$\mathrm{SNR} = \pi\left(\frac{Ax_m}{D}\right)^2 r_{\mathrm{K}} \tag{2.16}$$

with a single maximum at $D = 1/4$.

2.2 Linear response theory of SR

According to this theory the response of a nonlinear stochastic system $\langle x(t)\rangle$ to a weak external force $f(t)$ in the asymptotic limit of large times is determined by the integral relation [52, 54]

$$\langle x(t)\rangle = \langle x\rangle_{\mathrm{st}} + \int_{-\infty}^{\infty} \chi(t - \tau, D) f(\tau)\,\mathrm{d}\tau, \tag{2.17}$$

where $\langle x\rangle_{\mathrm{st}}$ is the mean value of the unperturbed state variable $[f(t) = 0]$ of the system, and $f(t)$ is the external disturbing force. Without lack of generality, we set $\langle x\rangle_{\mathrm{st}} = 0$ for simplicity. This condition holds for symmetric systems and, in particular, for the base model (2.1). The function $\chi(t)$ in (2.17) is called the response function and for systems which in the absence of perturbations are in thermodynamic equilibrium, is connected with the correlation functions of the unperturbed system via fluctuation-dissipation relations [58]. Let us discuss the application of linear response theory (LRT) to SR using the overdamped bistable system (2.1) as an example.

The fluctuation-dissipation theorem connecting the response function $\chi(t)$ and autocorrelation function $K_{xx}^{(0)}(t)$

of the unperturbed system has the form [50, 51]

$$\chi(t) = -\frac{1(t)}{D}\frac{\mathrm{d}}{\mathrm{d}t}K_{xx}^{(0)}(t)\,, \tag{2.18}$$

where $1(t)$ is the Heaviside function. In order to calculate the characteristics of the system response in the framework of LRT we need to know the statistical properties of the system in its unperturbed equilibrium or stationary state. For a harmonic force the system response is expressed through the susceptibility $\chi(\omega)$ which is a Fourier transform of the response function:

$$\langle x(t)\rangle = A\big|\chi(\omega)\big|\cos(\Omega t + \psi)\,, \tag{2.19}$$

where the phase shift ψ is given by

$$\psi = -\arctan\frac{\operatorname{Im}\chi(\Omega)}{\operatorname{Re}\chi(\Omega)}\,. \tag{2.20}$$

The SPA is defined as

$$\eta = \big|\chi(\omega)\big|^2\,. \tag{2.21}$$

The spectral density $G_{xx}(\omega)$ at the system output takes the form

$$G_{xx}(\omega) = G_{xx}^{(0)}(\omega) + \frac{\pi}{2}A^2\big|\chi(\Omega)\big|^2 \times\big[\delta(\omega-\Omega)+\delta(\omega+\Omega)\big] + \mathcal{O}(A^2)\,. \tag{2.22}$$

In the framework of this theory we can derive the SNR as follows

$$\mathrm{SNR} = \frac{\pi A^2\big|\chi(\Omega)\big|^2}{G_{xx}^{(0)}(\Omega)}\,. \tag{2.23}$$

It is impossible to get an exact expression for the autocorrelation function $K_{xx}^{(0)}(\tau, D)$. However, there are few approaches to its approximate evaluation. The most precise approach is based on the expansion of the Fokker – Planck operator in terms of eigenfunctions [32, 59]. The correlation function can be represented therewith as a series $g_j\exp(-\lambda_j\tau)$, where λ_j are the eigenvalues of the Fokker – Planck operator, and g_j are the coefficients which are computed by averaging the corresponding eigenfunctions over the unperturbed equilibrium distribution.

In the simplest case, when calculating the correlation function one may take into account a least nonvanishing eigenvalue λ_m that is related to the Kramers rate of the escape from a potential well:

$$\lambda_m = 2r_{\mathrm{K}} = \frac{\sqrt{2}}{\pi}\exp\left(-\frac{1}{4D}\right).$$

In this case the expressions for the correlation function and the spectral density of the unperturbed system are

$$K_{xx}^{(0)}(\tau, D) \approx \langle x^2\rangle_{\mathrm{st}}\exp(-\lambda_m\tau)\,, \tag{2.24}$$

$$G_{xx}^{(0)}(\omega) = \frac{2\lambda_m\langle x^2\rangle_{\mathrm{st}}}{\lambda_m^2+\omega^2} = \frac{2\sqrt{2}\pi\,\langle x^2\rangle_{\mathrm{st}}\exp(1/4D)}{2+\pi^2\omega^2\exp(1/2D)}\,, \tag{2.25}$$

where $\langle x^2\rangle_{\mathrm{st}}$ is the stationary value of the second cumulant of the unperturbed system

$$\langle x^2\rangle_{\mathrm{st}} = \int_{-\infty}^{\infty}x^2p_{\mathrm{st}}(x)\,\mathrm{d}x = C\int_{-\infty}^{\infty}x^2\exp\left[\frac{1}{D}\left(\frac{x^2}{2}-\frac{x^4}{4}\right)\right]\mathrm{d}x\,, \tag{2.26}$$

and C is the normalization constant for the stationary probability density. Such an approximation corresponds to the two-state approach and cannot be applied for small noise intensities ($D \ll 1$) and exposure to high-frequency external disturbance.

Allowance for the intrawell dynamics in the correlation function can be made by including an additional exponential term in expression (2.24), which describes fast fluctuations within potential wells. In this case the correlation function reflects both the global dynamics (factor λ_m) and the local intrawell dynamics [51, 57]:

$$K_{xx}^{(0)}(\tau, D) = g_1\exp(-\lambda_m\tau) + g_2\exp(-\alpha\tau)\,, \tag{2.27}$$

$$G_{xx}^{(0)}(\omega) = \frac{2\lambda_m g_1}{\lambda^2+\omega^2} + \frac{2\alpha g_2}{\alpha^2+\omega^2}\,, \tag{2.28}$$

where the factor α is derived from a linearized equation of motion, and $\alpha = |U''(x_{\min})|$, $x_{\min}$ is the coordinate of the potential minimum. For the particular example (2.1), $\alpha = 2$. The coefficients $g_{1,2}$ in formula (2.27) are determined from the expression for the correlation function and its derivative for $\tau = 0$ and are equal to [51]

$$\begin{aligned} g_1 &= \langle x^2\rangle_{\mathrm{st}} - g_2\,,\\ g_2 &= \frac{\lambda_m\langle x^2\rangle_{\mathrm{st}}}{\lambda_m-\alpha} + \frac{\langle x^2\rangle_{\mathrm{st}} - \langle x^4\rangle_{\mathrm{st}}}{\lambda_m-\alpha}\,,\\ \langle x^4\rangle_{\mathrm{st}} &= C\int_{-\infty}^{\infty}x^4\exp\left[\frac{1}{D}\left(\frac{x^2}{2}-\frac{x^4}{4}\right)\right]\mathrm{d}x\,. \end{aligned} \tag{2.29}$$

For the susceptibility in the two-state (single-exponent) approximation we obtain

$$\chi(\omega, D) = \frac{1}{D}\frac{\lambda_m\langle x^2\rangle_{\mathrm{st}}}{\lambda_m^2+\omega^2}(\lambda_m - \mathrm{i}\omega)\,, \tag{2.30}$$

and with regard to the intrawell dynamics

$$\chi(\omega, D) = \frac{1}{D}\left(\frac{g_1\lambda_m^2}{\lambda_m^2+\omega^2} + \frac{g_2\alpha^2}{\alpha^2+\omega^2}\right) - \mathrm{i}\omega\left(\frac{g_1\lambda_m}{\lambda_m^2+\omega^2} + \frac{g_2\alpha}{\alpha^2+\omega^2}\right). \tag{2.31}$$

Knowing the susceptibility and the spectral density of the unperturbed system one may find expressions for the SPA (3.5) and the SNR (6.37) [51, 57].

In order to study the amplitude-frequency properties of the system it is sufficient to consider the response to the harmonic signal $f(t) = A\cos(\Omega t)$. For the single-exponent approximation, the SPA and the SNR read as

$$\eta(\Omega, D) = \frac{1}{D^2}\frac{\big(\langle x^2\rangle_{\mathrm{st}}\lambda_m\big)^2}{\lambda_m^2+\Omega^2}\,, \tag{2.32}$$

$$\mathrm{SNR} = \frac{\pi A^2}{2D^2}\,\langle x^2\rangle_{\mathrm{st}}\lambda_m\,. \tag{2.33}$$

The result of the SNR is the same as in the two-state adiabatic theory [28]. Notice that the SNR (2.33) does not depend on the driving frequency and passes through a maximum at $D = 0.125$. The SPA η possesses a frequency dependence and, as seen from (2.32), is characterized by larger values in the low-frequency range.

Taking into account the intrawell dynamics, the SPA and the SNR assume the form [51]

$$\eta(\Omega, D) = \frac{(g_1\lambda_m)^2(\alpha^2+\Omega^2) + (g_2\alpha)^2(\lambda_m^2+\Omega^2) + 2g_1g_2\alpha\lambda_m(\alpha\lambda_m+\Omega^2)}{D^2(\lambda_m^2+\Omega^2)(\alpha^2+\Omega^2)}, \tag{2.34}$$

$$\mathrm{SNR} = \frac{\pi A^2}{2D^2} \times \frac{(g_1\lambda_m)^2(\alpha^2+\Omega^2) + (g_2\alpha)^2(\lambda_m^2+\Omega^2) + 2g_1g_2\alpha\lambda_m(\alpha\lambda_m+\Omega^2)}{g_2\alpha(\lambda_m^2+\Omega^2) + g_1\lambda_m(\alpha^2+\Omega^2)}. \tag{2.35}$$

The dependence of the amplification factor upon noise intensity is shown in Fig. 3a for different values of the external periodic signal frequency. As seen from the figure, both approximations yield similar results in the range of the maximal amplification [60].

The differences arise only for small noise intensities. The theory taking into account only the global dynamics of switchings between metastable states gives a vanishing η when $D \to 0$. The inclusion of the intrawell dynamics leads to the correct limit $\eta(\Omega, D \to 0) = 1/(\alpha^2+\Omega^2)$. In the limit $D \to 0$, the mean switching time from one potential well to another one becomes exponentially large and over a time equal to a great number of external force periods, the system is unable to switch from one state to the other. Hence, for small D the bistable oscillator behaves as a linear system with a characteristic time scale $1/\alpha$. When the driving frequency decreases, the maximum of the amplification shifts to the area of smaller noise intensities and the amplification factor itself increases. As follows from Fig. 3a, the amplitude-frequency characteristic of the system rises in the low-frequency region. This property follows from the physical nature of fluctuation processes in bistable systems where the noise energy is transformed into the low-frequency dynamics of stochastic switchings between metastable states. As a result, the fluctuation spectrum in the low-frequency range at the system output has a Lorentzian shape with a width governed by the mean Kramers rate of switching events.

The SNR (2.35) as a function of noise intensity is displayed in Fig. 3b. For small values of D, the SNR diverges and this fact can be explained by the contribution of the periodically modulated local dynamics inside the potential wells [28]. For sufficiently low driving frequencies the SNR achieves its maximum at $D \approx 1/8$. However, with increasing Ω, the SR effect disappears at all as the SNR becomes a monotonically decaying function of noise intensity.

3. Stochastic resonance for signals with a complex spectrum

In the majority of studies on SR the external force is a harmonic signal of a small amplitude. A natural problem arises to study the system response to multifrequency and noisy signals. This is especially important for biological and engineering applications. Signals recognized by living organisms are often noisy and may not contain strongly periodic components. The investigation of a system's response to the quasi-harmonic signal with a finite spectral linewidth, resulted from the fluctuation contribution, seems to be more realistic.

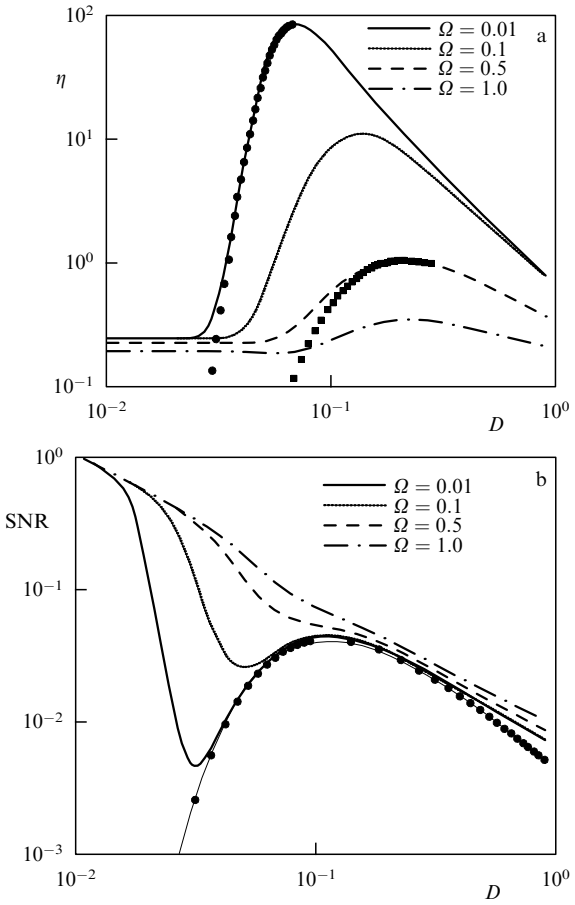

Figure 3. (a) Spectral power amplification η (2.34) and (b) the signal-to-noise ratio (2.35) as functions of the noise intensity D for different values of the external periodic signal frequency. The dependences (2.32), (2.33) obtained without regard to the intrawell dynamics are shown by symbols •.

An advantage of LRT is that it can be naturally extended to the case of signals with a complex spectral composition. The spectral density at the output takes the form

$$G_{xx}(\omega) \approx G_{xx}^{(0)}(\omega) + \left|\chi(\omega)\right|^2 G_{ff}(\omega), \tag{3.1}$$

where $G_{ff}(\omega)$ is the spectrum of the signal. Below we shall discuss a series of examples which are of practical importance.

3.1 Response of a stochastic bistable system to multifrequency signal

Let us consider a weak signal possessing a discrete spectrum. The external force $f(t)$ can be represented in the form of a Fourier series

$$f(t) = A\sum_{k=1}^{M} c_k \cos\Omega_k t, \tag{3.2}$$

where $Ac_k \ll 1$ are the small amplitudes of the harmonics, and Ω_k are their frequencies. According to LRT the system response reads as

$$\langle x(t)\rangle = A\sum_{k=1}^{M} c_k\left|\chi(\Omega_k, D)\right|\cos\left[(\Omega_k+\psi_k)t\right]. \tag{3.3}$$

The response $\langle x(t)\rangle$ (3.3) contains the same spectral components (3.2) but with different amplitudes and phases. In Eqn

(3.3), phase shifts ψ_k for each harmonic are given via the susceptibility as

$$\psi_k(\Omega_k, D) = -\arctan\frac{\operatorname{Im}\chi(\Omega_k, D)}{\operatorname{Re}\chi(\Omega_k, D)}\,. \tag{3.4}$$

In accordance with the linear response theory, SR measures, such as the SPA and the SNR, are determined as follows [51, 55]

$$\eta(\Omega_k, D) = \left|\chi(\Omega_k, D)\right|^2, \tag{3.5}$$

$$\mathrm{SNR}(\Omega_k, D) = \frac{\pi(Ac_k)^2|\chi(\Omega_k, D)|^2}{G_{xx}^{(0)}(\Omega_k, D)}\,. \tag{3.6}$$

The frequency dependence of the susceptibility provides frequency distortions of the output signal. In order to estimate the magnitudes of those distortions one can use the ratio of the amplitudes of different harmonics at the output to the same ratio at the input

$$E(\Omega_k, \Omega_j, D) = \frac{\left|\chi(\Omega_k, D)\right|}{\left|\chi(\Omega_j, D)\right|}\,. \tag{3.7}$$

As follows from Eqns (2.32)–(2.35), an overdamped bistable oscillator (2.1) represents an amplifier with low-frequency filtering of the signal at the output. The parameters of such an amplifier (the SPA and the SNR) are controlled by the intensity of an external noise. The question arises: is it possible, using such a device, to provide amplification of information-carrying signals (for instance, amplitude and frequency modulated signals) without significant distortions? This problem has been discussed in Refs [60–62], where a positive answer has been given to this question. If the conditions of SR are effected in the weak-signal approximation and if its effective frequency range does not exceed 25% of the carrier frequency, then all the frequency components of the signal will be amplified almost similarly and the output signal will contain practically no linear distortions.

3.2 Stochastic resonance for signals with a finite spectral linewidth

Actual periodic signals always possess a finite spectral linewidth due to the presence of amplitude and phase fluctuations of the oscillator [1–3, 63]. Will SR be observed for such signals and which features may it lead to if one takes into account the finite width of the spectral line? The answer to these questions is of great importance in practical applications [38, 50].

As a model of a signal with a finite spectral linewidth we took [38] so-called 'harmonic noise' [64]. Harmonic noise is represented by a two-dimensional Ornstein–Uhlenbeck process and is governed by the set of two stochastic differential equations

$$\dot{y} = s\,, \qquad \dot{s} = -\Gamma s - \Omega^2 y + \sqrt{2\epsilon\Gamma}\,n(t)\,, \tag{3.8}$$

where $n(t)$ is a Gaussian white noise, $\langle n(t)n(t')\rangle = \delta(t-t')$, Γ is the parameter of dissipation, and ϵ is the intensity of harmonic noise. The spectral density $G_{yy}(\omega)$ is a Lorentzian one

$$G_{yy}(\omega) = \frac{2\epsilon\Gamma}{\omega^2\Gamma^2 + (\omega^2 - \Omega^2)^2}\,. \tag{3.9}$$

For $\Omega > \Gamma/2$, the spectral density (3.9) possesses a peak at the frequency

$$\omega_{\mathrm{p}} = \sqrt{\Omega^2 - \frac{\Gamma^2}{2}} \tag{3.10}$$

and is characterized by the FWHM $\Delta\omega_{\mathrm{in}}$ determined at the half height of the peak maximum:

$$\Delta\omega_{\mathrm{in}} = \sqrt{\omega_{\mathrm{p}}^2 + \Gamma\omega_1} - \sqrt{\omega_{\mathrm{p}}^2 - \Gamma\omega_1}\,, \qquad \omega_1 = \sqrt{\Omega^2 - \frac{\Gamma^2}{4}}\,. \tag{3.11}$$

It has been shown that for the case of a signal with a finite spectral linewidth the SR effect can also be realized. Moreover, it has been established that the width of the spectral line at the output of a bistable system can be reduced at an optimal noise intensity [39].

3.3 Aperiodic stochastic resonance

As has been already mentioned, the spectra of signals recognized by biological systems are very complicated. Can SR be observed for such signals and what is its mechanism? The answer to the first question is positive and was given in Refs [65, 66] using neuron models. This kind of SR was called aperiodic. It this section we shall show that aperiodic SR can be described in the framework of LRT [67, 68].

In the case of an aperiodic signal having no peaks in its spectrum the measures used for conventional SR (the SPA, the SNR, and the residence-time distribution) are either inapplicable or ineffective. The quantities characterizing the transmission of a noisy signal through a system can be computed on the basis of the cross-correlation functions (or mutual spectral densities) between the input and output of the system [110]. We suppose that an input signal $s(t)$ applied to the system gives rise to a stochastic process at the output $x(t)$. Let us treat $s(t)$ and $x(t)$ as stationary stochastic processes. As is known, the cross-correlation function $K_{xs}(\tau)$ of the processes $s(t)$ and $x(t)$ is defined as

$$K_{xs}(\tau) = \int_{-\infty}^{\infty}\int_{-\infty}^{\infty} xsp(x, t;\, s, t+\tau)\,\mathrm{d}x\,\mathrm{d}s\,, \tag{3.12}$$

where $p(x, t;\, s, t+\tau)$ is the two-dimensional joint probability density of $s(t)$ and $x(t)$ processes. The mutual spectral density is a Fourier transform of the cross-correlation function, i.e.

$$G_{xs}(\omega) = \int_{-\infty}^{\infty} K_{xs}(\tau)\exp(-\mathrm{i}\omega\tau)\,\mathrm{d}\tau\,. \tag{3.13}$$

Let us introduce the coherence function $\Gamma(\omega)$ in the following way:

$$\Gamma^2(\omega) = \frac{\left|G_{xs}(\omega)\right|^2}{G_{xx}(\omega)G_{ss}(\omega)}\,. \tag{3.14}$$

This quantity varies on the closed interval $[0, 1]$ and governs the degree of linear coherence of $x(t)$ and $s(t)$ processes at the frequency ω.

Let a stochastic system be characterized by the susceptibility $\chi(\omega, D)$, where D is the internal noise intensity. The signal $s(t)$ is assumed to be weak. Suppose also that $s(t)$ is a Gaussian stationary stochastic process statistically indepen-

dent of the internal noise of the system. The statistical characteristics of the system response to the external signal $s(t)$ can be computed via LRT [68, 69]. For the mutual spectral density $G_{xs}(\omega)$ we have

$$G_{xs}(\omega) = \chi(\omega, D) G_{ss}(\omega) . \tag{3.15}$$

The spectral density at the output reads as

$$G_{xx}(\omega) \approx G_{xx}^{(0)}(\omega, D) + \left|\chi(\omega, D)\right|^2 G_{ss}(\omega) , \tag{3.16}$$

where $G_{xx}^{(0)}(\omega, D)$ is the spectral density of the unperturbed system without driving signal. Inserting Eqns (3.15), (3.16) into Eqn (3.14) we derive the coherence function in the linear response approximation:

$$\Gamma^2(\omega) = 1 - \frac{G_{xx}^{(0)}(\omega, D)}{G_{xx}^{(0)}(\omega, D) + \left|\chi(\omega, D)\right|^2 G_{ss}(\omega, D)} . \tag{3.17}$$

As seen from this formula, the coherence function is always less than 1 and depends on the internal noise intensity D. As has been shown in Ref. [68], the degree of coherence between input and output is optimal at a certain noise level. As the correlation time of the signal increases, the coherence of the input and the output enhances. Hence, aperiodic SR is described in the framework of general LRT in a similar manner to the case of a periodic signal.

4. Nondynamical stochastic resonance. Stochastic resonance in chaotic systems

In the previous section the main attention was paid to the properties of SR depending on the structure of the input signal. Specific nature of the dynamical system was not of principal importance. However, both the qualitative and quantitative SR features also depend on the particular type of system which is used as a stochastic resonator. If we interpret SR as a noise-induced enhancement of the coherence between the output and input of a device, then this effect can be realized in monostable nonlinear oscillators and even in nondynamical (threshold) systems. SR is also observed in chaotic systems demonstrating bistability in the sense of noise-induced or purely dynamical intermittency.

In the present section we study SR effects whose mechanisms and properties are mainly determined by the type of system and its behaviour.

4.1 Stochastic resonance as a fundamental threshold phenomenon

From the point of view of the transmission of information (signal) through bistable systems in the regime of SR, the transitions over a potential barrier play a major role, while the local intrawell dynamics is not important. Therefore, in output signal processing the two-state approach is used successfully. The output is interpreted as a random telegraph process in which a periodic component of the fundamental frequency is extracted via filtering. We may abandon altogether the analysis of bistable dynamical systems and treat stochastic resonance as a fundamental threshold effect. In this case the act of transmitting is considered to be a sequence of random events occurring when the sum of regular and noisy components of the input signal intersects a given threshold C_{th}:

$$\left[B \sin \omega t + \xi(t)\right] > C_{\text{th}} \quad \text{or} \quad < C_{\text{th}} . \tag{4.1}$$

We examine SR using a conception of the nondynamical threshold effect [36]. Instead of dynamic equations we establish a set of rules as indicated in Fig. 4. Figure 4a represents a subthreshold regular signal $B \sin \omega t$ and additive noise $\xi(t)$. In the absence of noise the signal amplitude B is inadequate to achieve the threshold $C_{\text{th}} = A$. When the noise is added, the threshold is crossed and this occurs randomly.

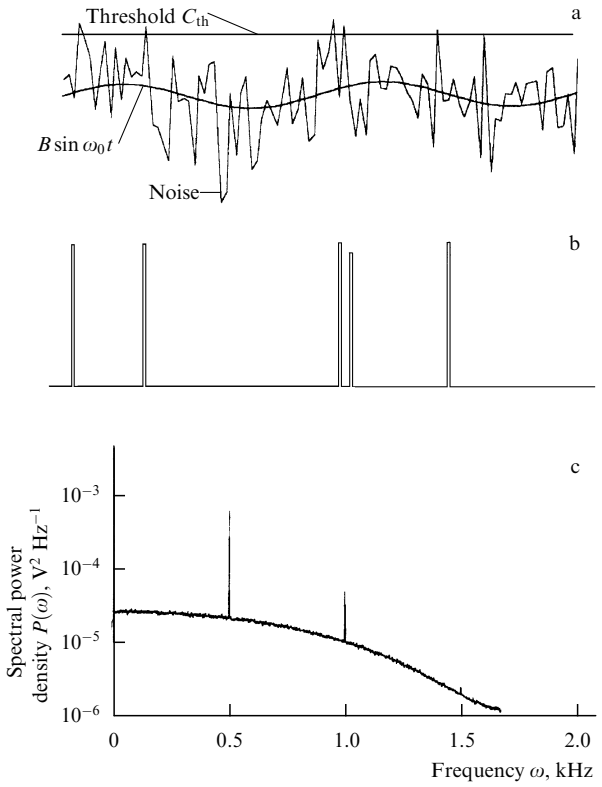

Figure 4. (a) Sinusoidal subthreshold signal plus noise; (b) threshold crossings are marked by a sequence of standard pulses; (c) the power spectrum of the pulse train.

Each time the threshold is crossed in one direction, a pulse of a standard shape is generated. Thus, the threshold crossing events give rise to a train of random-in-time pulses as shown in Fig. 4b. The power spectrum of such a pulse train is shown in Fig. 4c. This power spectrum is similar to that for a bistable oscillator, except that it contains all the harmonics $n\omega$ of the fundamental frequency. The SNR can be determined from the power spectrum in the same manner as before. The dependence of the SNR upon noise intensity demonstrates the SR effect.

Threshold SR admits a simple theoretical description under the following assumptions: (1) we use the standard limitation of the adiabatic theory: $\omega \ll \langle \nu \rangle$, where $\langle \nu \rangle$ is the mean threshold crossing rate; (2) we assume the pulses to be uncorrelated, and (3) the width of the pulses τ is assumed to be limited and is negligibly small compared to the mean threshold crossing time, i.e. $\tau \ll \langle \nu \rangle^{-1}$.

The nondynamical theory of SR is based on a classical formula for the mean threshold crossing rate $\langle \nu \rangle$ and the assumption that the noise $\xi(t)$ shows evidence of being the Gaussian band-limited process with a cutoff frequency

f_0 [70]:

$$\langle \nu \rangle = \frac{g(\Delta)}{g(0)} \left[\frac{\int f^2 S(f)\, \mathrm{d}f}{\int S(f)\, \mathrm{d}f} \right]^{1/2} = \frac{g(\Delta) f_0}{\sqrt{3}\, g(0)}\,, \tag{4.2}$$

where Δ is the threshold, f_0 is the cutoff frequency of a low-frequency filter, and $g(\Delta)/g(0)$ is the Gaussian function

$$\frac{g(\Delta)}{g(0)} = \exp\left(-\frac{\Delta^2}{2\sigma^2}\right), \tag{4.3}$$

where σ^2 is the noise variance.

If each threshold crossing event gives rise to a rectangular pulse of width τ and amplitude A, and if we assume that $\tau \ll \langle \nu \rangle^{-1}$ and the pulses are uncorrelated, then according to Campbell's theorem the power spectrum of the pulse train is

$$P_{\mathrm{N}}(f) \simeq \frac{1}{2}\, A^2 \tau^2 \langle \nu \rangle = \frac{1}{2}\, A^2 \tau^2 \left(\frac{f_0}{\sqrt{3}}\right) \exp\left(-\frac{\Delta^2}{2\sigma^2}\right). \tag{4.4}$$

Expression (4.4) characterizes the uniform noise spectrum. Although the actual power spectrum is a slowly decaying function of frequency (see Fig. 4c), Eqn (4.4) can be used as an estimate of the power spectrum in a low-frequency range. The mean amplitude of the random pulse train is

$$\langle V \rangle = A\tau \langle \nu \rangle = A\tau \left(\frac{f_0}{\sqrt{3}}\right) \exp\left(-\frac{\Delta^2}{2\sigma^2}\right). \tag{4.5}$$

We now add the small periodic signal $B \sin \omega t$ that causes the threshold to be modulated with the frequency ω: $\Delta \to \Delta_0 + B \sin \omega t$. As a result, the mean threshold crossing rate $\langle \nu \rangle$ and the mean amplitude $\langle V \rangle$ of the pulse train studied also become time-dependent:

$$\begin{aligned} \langle V \rangle(t) &= \frac{A\tau f_0}{\sqrt{3}} \exp\left[-\frac{1}{2\sigma^2}\left(\Delta_0^2 + 2\Delta_0 B \sin \omega t + B^2 \sin^2 \omega t\right)\right] \\ &\simeq \frac{A\tau f_0}{\sqrt{3}} \left(1 - \frac{B^2}{4\sigma^2} - \frac{\Delta_0 B}{\sigma^2} \sin \omega t + \frac{B^2}{4\sigma^2} \cos 2\omega t\right), \end{aligned} \tag{4.6}$$

where we have used the simplifying condition $B \ll \sigma\Delta_0$. Calculating the Fourier transform we obtain the power spectrum of the signal with delta-peaks at frequencies ω and 2ω:

$$P_{\mathrm{S}}(f) = \frac{A^2 \tau^2 f_0^2}{3} \left[\left(\frac{\Delta_0 B}{\sigma^2}\right)^2 \delta(\omega) + \left(\frac{B^2}{4\sigma^2}\right)^2 \delta(2\omega) \right] \exp\left(-\frac{\Delta_0^2}{\sigma^2}\right). \tag{4.7}$$

For the signal with a fundamental frequency ω we can calculate the SNR using the well-known definition:

$$\mathrm{SNR} = 10 \lg \left(\frac{2 f_0 \Delta_0^2 B^2}{\sigma^4 \sqrt{3}}\right) \exp\left(-\frac{\Delta_0^2}{2\sigma^2}\right). \tag{4.8}$$

The dependence of the SNR on the standard deviation σ is typical for SR.

We note that this simple and approximate theory captures the basic features of the effect under consideration and is in qualitative agreement with experimental and simulated data. A more detailed and accurate theory of nondynamical SR has been developed in Ref. [37].

4.2 Stochastic resonance in chaotic systems

The situation when attractors of different types coexist in the phase space is typical for systems demonstrating dynamical chaos [71]. Without external noise a phase trajectory belongs to either one or another attractor depending on the initial conditions. The influence of external noise leads to the appearance of random switchings between coexisting attractors of the system. The statistics of these switchings is defined by the properties of the noise and the dynamical system.

A theoretical consideration of the influence of external noise on the regimes of dynamical chaos is available in the limits of small [72–74] and large [75] Gaussian noise. The theory of random perturbations of dynamical systems [76] is based on the notion of a quasi-potential and has been recently extended to systems with complex dynamics [77, 78]. Suppose that a dynamical system has an attractor and for this object there exists an invariant probabilistic measure. Let the system be subjected to a weak Gaussian noise with intensity D and be described by the set of stochastic differential equations (SDE)

$$\dot{x}_i = f_i(x) + \xi_i(t)\,, \qquad i = 1, \ldots, N\,, \tag{4.9}$$

where $\left\langle \xi_i(t) \xi_j(0) \right\rangle = 2D\delta_{i,j}\delta(t)$. Then the stationary probability density $p(x)$ can be written via the quasi-potential $\Phi(x)$ as follows

$$p(x) \propto \exp\left[-\frac{\Phi(x)}{D}\right]. \tag{4.10}$$

The quasi-potential, being an analogue of the free energy for the nonequilibrium stationary state [63, 79], depends only on state variables and parameters of the system and does not depend on the intensity D. The quasi-potential takes the minimal values on the attractor. If a few attractors coexist in the phase space of the system, then $\Phi(x)$ possesses local minima corresponding to these attractors, and in the presence of weak noise we may formulate the Kramers problem. For $D \ll 1$, the motion of the system involves a slow time scale related to the mean time of escape from the attraction basin of an attractor. The dependence of the mean escape time upon the noise intensity is characterized by the exponential law $v(D) \exp(\Delta\Phi/D)$. If additionally to external noise we apply a weak periodic signal to the system, which cannot evoke transitions in the attraction basins of other attractors, the phenomenon of SR has a right to be observed [34, 35].

A principally different effect called *deterministic stochastic resonance* has been recently revealed for systems with chaotic dynamics [34, 35]. With the variation of control parameters of a chaotic system a crisis of its attractors may occur. As an example we can mention here the phenomenon of two attractors merging leading to a 'chaos–chaos' dynamical intermittency [80]. In this case a phase trajectory spends a long time on each of the merged attractors and rarely makes irregular transitions between them. We note that such randomlike switchings occur in the absence of external noise and are controlled via the deterministic law [81, 82]. For the systems with a 'chaos-chaos' intermittency, the mean residence time T_i of a phase trajectory to be on an attractor obeys an universal scaling law [80–83]

$$T_i \propto (a - a_{\mathrm{cr}})^{\gamma}\,, \tag{4.11}$$

where a is a control parameter, a_{cr} is its bifurcation value at which a crisis occurs and corresponds to the onset of

intermittency, and γ is the scaling exponent. Hence, in this case the control parameter plays the role of noise intensity. It controls a slow time scale, the mean residence time, and, consequently, the spectral properties of the system [83]. If the system is driven by a periodic signal via variation of this parameter, we can obtain a situation when the driving period and the mean time of switching from one attractor to the other coincide, i.e. the conditions of SR are realized. Notice that the regimes of dynamical intermittency exhibit an exponential sensitivity to external noise [82, 83] that makes possible a realization of the conventional SR.

We shall illustrate deterministic SR using a simple example of a discrete system:

$$x_{n+1} = (ax_n - x_n^3)\exp\left(-\frac{x_n^2}{b}\right) + A\sin\omega n + \sqrt{2D}\,\xi(n)\,. \quad (4.12)$$

The system (4.12) is the one-dimensional cubic map perturbed by a weak periodic signal ($A \ll 1$) and a delta-correlated noise of intensity D. The exponential term is introduced in order to prevent escapes of phase trajectories to infinity.

Let us describe originally the behaviour of the unperturbed map ($A = D = 0$). At $a < a_{\rm cr} = 2.839\ldots$, two chaotic attractors are separated by the saddle point $x_n = 0$ and coexist in the phase space of the system. At $a = a_{\rm cr}$, these attractors merge with the onset of dynamical intermittency of 'chaos–chaos' type.

First we study conventional SR before the crisis $a < a_{\rm cr}$ when the switching events are due to external noise. Figure 5a displays the dependences of the SPA and the SNR on the intensity of an external noise D. Both the SPA and the SNR pass through maxima at optimal noise levels. Simulations have confirmed that the Kramers rate is close to the external signal frequency at the optimal noise intensity $D = D_{\rm opt}$.

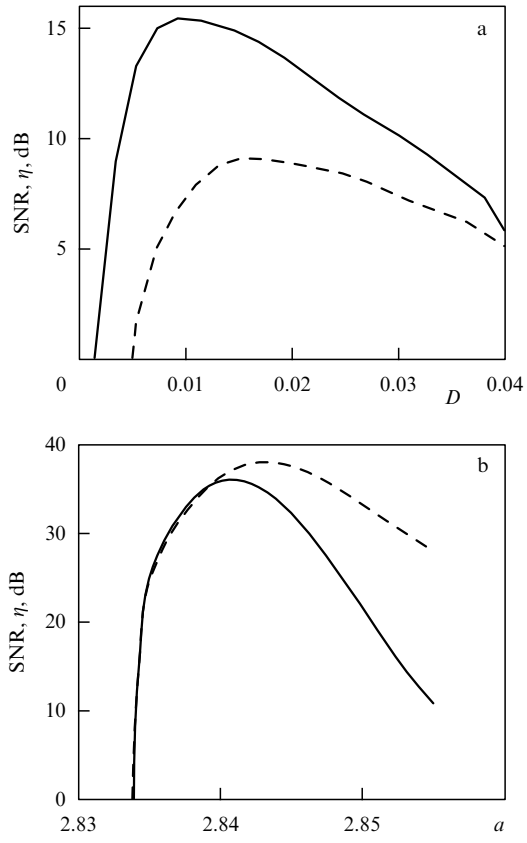

Figure 5. SNR (solid line) and SPA (dashed line) as functions of the noise intensity D (upper: $a = 2.5$, $A = 0.05$, $\omega = 0.1$) and of the control parameter a (lower: $D = 0$, $A = 0.005$, $\omega = 0.1$).

Now we exclude noise ($D = 0$) and consider the system's reaction to periodic disturbance in a regime when the parameter a is slightly larger than its critical value, $a > a_{\rm cr}$. According to simulations, the mean switching frequency monotonically increases with increasing parameter a. Figure 5b shows the dependences of the SPA and the SNR on a. The graphs illustrate the effect of deterministic SR, i.e. maxima of the SPA and the SNR can be obtained by tuning the control parameter in the range $2.85 < a < 2.88$, when the Kramers rate matches the external signal frequency.

The effects described above have a generic character, which was verified by numerical simulations of various discrete and flow systems demonstrating both noise-induced intermittency and a crisis [34]. As an example we discuss SR in the Lorenz model in the regime of noise-induced intermittency. The Lorenz system [84] is a suitable model for studying the influence of noise on the chaotic dynamics [85–88] since noise sources can be included into the equations of motion using fluctuation-dissipation relations. A stochastic Lorenz model is described by the following system of SDE:

$$\begin{aligned}
&\dot{x} = -\sigma x + \sigma y + \xi_1(t)\,,\\
&\dot{y} = -y + rx - xz + \xi_2(t)\,,\\
&\dot{z} = -bz + xy + \xi_3(t)\,,\\
&\langle \xi_i(t)\xi_j(0)\rangle = D\,\delta_{i,j}\,\delta(t)\,.
\end{aligned} \quad (4.13)$$

Over the region of the parameter values $\sigma = 10$, $r = 210$, $b = 8/3$, corresponding to the existence of a quasi-attractor, there are two symmetric chaotic attractors in the phase space of the noise-free system. Noise induces 'chaos-chaos' intermittent behaviour of switchings between these attractors [88].

Neglecting the local chaotic dynamics on these attractors and taking into consideration switchings only between them (the two-state approximation), the correlation function exponentially decreases: $K_{xx}(\tau) \propto \exp\bigl[-2r(D)\bigr]$, where $r(D)$ is the mean escape rate from the effective potential well. In this way the susceptibility of the Lorenz system can be estimated by the same expression as for an overdamped bistable oscillator.

Let us add a weak periodic signal $A\sin\Omega t$ to the first equation of the set (4.13). In this case the spectral density will contain a delta-peak at the signal frequency.

The simplest estimate for the SNR at the system output is

$$\mathrm{SNR} \propto \frac{r(D)}{D^2} = \frac{1}{D^2}\exp\left(-\frac{\Delta\Phi}{D}\right), \quad (4.14)$$

where $\Delta\Phi$ is the barrier height of the corresponding effective potential. Numerical calculations of the SNR based on Eqns (4.13) are in good agreement with this theoretical estimate. Therefore, the expression for the SNR (4.14) is a rather universal one, which describes the SNR for simple bistable systems as well as for systems with complex dynamics. Notice that the Lorenz model can be transformed into the form of a bistable oscillator with inertial nonlinearity [71, 89]:

$$\ddot{u} + \gamma\dot{u} + u^3 + (v-1)u = 0\,, \qquad \dot{v} = h(\beta u^2 - \alpha v)\,, \quad (4.15)$$

where $\gamma=(1+\sigma)/\sqrt{\sigma(r-1)}$, $h=(r-1)^{-1/2}$, $\beta=(2\sigma-b)/\sqrt{\sigma}$, and $\alpha=b/\sqrt{\sigma}$. For large values $r\gg 1$, variable $v(t)$ is slow and after excluding it from (4.15) we arrive at the equation for a bistable oscillator no longer containing the nonlinear inertial term:

$$\ddot{u}+\gamma\dot{u}+\frac{\alpha+\beta}{\alpha}\,u^3-u=0\,. \tag{4.16}$$

Therefore, in the limit of large r the Lorenz system can be described in terms of a bistable oscillator, and this fact guarantees the existence of SR.

5. Synchronization of stochastic systems

An application of the linear response theory yields good results explaining the physical mechanism of the SR phenomenon. The question arises, why? We know that all stochastic systems demonstrating SR are essentially nonlinear! The reason is that the fundamental nonlinear properties of stochastic systems are taken into account, in one approximation or another, when defining the correlation function of the unperturbed system. The nonlinearity of the system manifests itself in the dependence of the correlation function on the noise intensity D. As a result, the susceptibility also depends on D. The limitations of LRT lead to the requirement for the amplitude of the disturbing signal to be extremely small. Refusing this condition we shift the problem to a class of principally nonlinear problems where LRT is no longer valid.

One of the important nonlinear effects accompanying SR is synchronization. The synchronization of stochastic systems, which do not have any natural periodic components in time series pertaining to the process realizations, is considered to be a nontrivial phenomenon. Recently effects of forced [90–93] and mutual [94] stochastic synchronization have been reported.

5.1 Synchronization of a stochastic bistable oscillator

In order to consider the synchronization effect in stochastic systems we turn to the results obtained for the van der Pol nonautonomous oscillator, which is a classical autooscillating system with an isolated closed phase curve, driven by a periodic force and noise [1–3]. As is known, noise causes fluctuations of the oscillation amplitude and phase. As a result, the oscillation phase difference $\phi(t)=\Phi(t)-\Psi(t)$ of the oscillator, $\Phi(t)$, and the external harmonic force, $\Psi(t)$, also fluctuates. The stochastic dynamics of $\phi(t)$ for the synchronized van der Pol oscillator can be qualitatively described by the following SDE [1]:

$$\dot{\phi}=\Delta-\epsilon\sin\phi+\xi(t)\,, \tag{5.1}$$

where $\Delta=\Omega-\Omega_0$ is the frequency mismatch of the oscillator and the external force (a frequency detuning), ϵ is the parameter of nonlinearity, $\xi(t)$ is the Gaussian noise and the amplitude fluctuations are neglected. As follows from Eqn (5.1), the phase difference $\phi(t)$ executes Brownian motion in a tilted periodic potential $U(\phi)=-\Delta\phi-\epsilon\cos\phi$. If the noise intensity is small, the phase difference fluctuates for a long time inside one of the potential wells (that means phase locking) of $U(\phi)$ and rarely jumps over the potential barrier (loss of synchronization), demonstrating phase slips.

In contrast to a clear definition of the synchronization process for deterministic systems, the notion of synchronization is ambiguous for systems with noise and we have to use in that case the notion of an *effective synchronization*. It can be defined by imposing restrictions on (i) phase fluctuations, (ii) frequency fluctuations, and (iii) the signal-to-noise ratio [3]. We give here the strongest definition of effective synchronization: a system is effectively synchronized by a periodic force if the mean time of phase locking is much greater than a period of external harmonic force. A quantity which can be used as a measure of effective synchronization is the effective diffusion coefficient of the phase difference:

$$D_{\text{eff}}=\frac{1}{2}\,\frac{\mathrm{d}}{\mathrm{d}t}\left[\left\langle\phi^2(t)\right\rangle-\left\langle\phi(t)\right\rangle^2\right]. \tag{5.2}$$

It can be shown that D_{eff} is proportional to the mean rate r of escape from a well of periodic potential $U(\phi)$, i.e. $D_{\text{eff}}=4\pi^2 r$, and is inversely proportional to the mean time of phase locking (or the mean interval between phase slips) $\langle T\rangle=n2\pi/\Omega_0$, $n\gg 1$ [1]. Therefore, we can define the criterion of effective synchronization as

$$D_{\text{eff}}\leqslant 2\pi\,\frac{\Omega_0}{n}\,,\qquad n\gg 1\,, \tag{5.3}$$

where n is an integer ($n=1,2,\ldots$). This condition guarantees that the phase is locked for at least n periods of the driving force. The influence of additive noise on a synchronized self-excited oscillator is well studied [1–3]: the effective diffusion coefficient grows with increasing noise intensity as the synchronization conditions are impaired in the process. Synchronization regions (for instance, Arnold's tongues) in the parameter space of the system contract with enhancing noise [100, 101]. In other words, noise acts against synchronization by causing disorder (stochastic phase diffusion). We will show further that in SR systems noise plays a radically different role.

Let us go back again to the basic model of the overdamped bistable oscillator and write its SDE as follows

$$\dot{x}=\alpha x-\beta x^3+\sqrt{2D}\,\xi(t)+A\cos(\Omega_0 t+\psi_0)\,. \tag{5.4}$$

The system governed by Eqn (5.4) does not possess any natural deterministic frequency, but is characterized by a noise-controlled time scale, i.e. the mean time of escape from a potential well, which is matched by the mean switching frequency in the frequency domain. A periodic signal represents something like an external 'clock' with respect to the bistable oscillator. The interesting question arises: is this external clock amenable to effectively synchronize the switching events in the stochastic bistable system? Although at first sight it may look strange, the answer is positive. Now we pass to the proof.

We assume that in SDE (5.4) $\alpha,\beta>0$; $\psi_0=0$ and the modulation amplitude A is small compared to the potential barrier:

$$A<A_0=\frac{2}{3}\left(\frac{\alpha^3}{3\beta}\right)^{1/2}. \tag{5.5}$$

Besides, we suppose that the modulation frequency is also small and the adiabatic approximation may be applied.

In order to introduce the notion of an instantaneous phase of an aperiodic signal we need to use the concept of an analytic signal [95–99]. The analytic signal $w(t)$ is a complex function of time defined as [96]

$$w(t)=x(t)+\mathrm{i}y(t)=a(t)\exp\left[\mathrm{i}\Phi(t)\right], \tag{5.6}$$

where $y(t)$ is the Hilbert transform of the original process $x(t)$:

$$y(t) = \frac{1}{\pi}\int_{-\infty}^{\infty} \frac{x(\tau)}{t-\tau}\, \mathrm{d}\tau\,. \tag{5.7}$$

In the latter expression the integral is taken in the sense of the Cauchy principal value. For a stochastic process $x(t)$, the integral converges in the mean square sense. The instantaneous amplitude $a(t)$ and the phase $\Phi(t)$ of $x(t)$ are defined as

$$a^2(t) = x^2(t) + y^2(t)\,, \qquad \Phi(t) = \arctan\frac{y(t)}{x(t)}\,, \tag{5.8}$$

as well as the instantaneous frequency $\omega(t) = \mathrm{d}\Phi(t)/\mathrm{d}t$ is written in the following way

$$\omega(t) = \frac{1}{a^2(t)}\left[x(t)\dot{y}(t) - y(t)\dot{x}(t)\right]. \tag{5.9}$$

Afterwards, the mean frequency $\langle\omega(t)\rangle$ is given by

$$\langle\omega\rangle = \lim_{T\to\infty}\frac{1}{T}\int_0^T \omega(t)\,\mathrm{d}t\,. \tag{5.10}$$

Finally, we introduce the instantaneous phase difference between the output and input signals as

$$\phi(t) = \Phi(t) - \Omega_0 t\,. \tag{5.11}$$

The above-used concept of the analytic signal gives the most general definition of the instantaneous amplitude and phase, which is not unique. Generality is understood in the sense that definitions (5.9)–(5.11) take into account both the local intrawell dynamics and global transitions between the potential wells. From the other side, as research has shown, the basic information on the processes in the system is contained in a sequence of switching times and can be studied by the method of two-state dynamics described above. In this connection it is worth introducing an alternative definition of the phase, which would be equivalent to a simplified consideration with the intrawell dynamics excluded. Following Ref. [30] let us consider only switching events. For this purpose we map the continuous stochastic process $x(t)$ onto a stochastic point process t_k, where t_k are the times when a Brownian particle crosses the potential barrier. The residence time between two subsequent switching events is then $T(t) = t_{k+1} - t_k$, $t_k < t < t_{k+1}$. The corresponding dichotomic process $u(t)$ can be described by the equation

$$u(t) = x_m \operatorname{sgn}\left[\cos\Phi(t)\right], \tag{5.12}$$

where x_m is the distance between the potential barrier and a minimum of the potential wells of the system defined by Eqn (5.4), and $\Phi(t)$ is the phase specified as

$$\Phi(t) = \pi\,\frac{t-t_k}{t_{k+1}-t_k} + \pi k\,, \qquad t_k < t < t_{k+1}\,. \tag{5.13}$$

Hence, the phase defined in this way is a piecewise-linear function of time and gives an exact description of phase when transitions between metastable states of the system are in full synchrony with the external force, i.e. with the period $2\pi/\Omega_0$. The instantaneous frequency between the switchings is constant and equals $\pi/T(t)$. According to this phase definition, the mean frequency reads as

$$\langle\omega\rangle = \lim_{M\to\infty}\frac{1}{M}\sum_{k=1}^{M}\frac{\pi}{t_{k+1}-t_k}\,, \tag{5.14}$$

and is equivalent to the mean switching frequency of the system [90].

Notice that both definitions of the instantaneous phase lead to equivalent results after averaging.

Phase synchronization. Time series of the instantaneous phase difference calculated using the analytic signal representation are shown in Fig. 6a for different noise intensities D. It is seen that there is an optimal value $D = 0.80$ at which the phase difference remains constant over a long time interval, i.e. we observe the external noise-controlled effect of switching frequency forced synchronization in the bistable stochastic system. Forced synchronization can be detected in the same manner using the second definition for the phase (5.13). The mean frequencies against noise intensity are shown in Fig. 6b for different values of the modulation amplitude. The data were obtained using both definitions (5.6)–(5.10) and (5.14) and clearly demonstrate the effect of mean switching frequency locking first reported in Ref. [90]. This figure displays both the existence of a synchronization threshold and the expansion of the synchronization region with increasing modulation amplitude. Without external force ($A = 0$) the mean frequency monotonically grows following Kramers law. For $A \geqslant 1$, the dependence $\langle\omega\rangle(D)$ shows a slightly marked bend; at $A = 2$ we can clearly see a 'plateau' where $\langle\omega\rangle$ no longer depends on D. As the amplitude increases further, $A = 3$, the synchronization zone is expanded [93].

In accordance with the definition of effective synchronization, we need to calculate the effective diffusion coefficient (5.2). The results are shown in Fig. 6c. As seen from the figure, as the driving amplitude goes up, the dependences of D_{eff} on the noise intensity are characterized by more and more clearly marked minima. Quantitative values of D_{eff} in the synchronization region indicate that the effect of frequency and phase locking occurs over the time intervals which are about 10^3 times as long as the driving period. According to the definition given above we can ascertain the presence of effective synchronization at the fundamental tone manifesting itself in phase and frequency locking by an external signal. A nontrivial fact here is that an additional noise applied to the system causes the phase dynamics of the system to be more ordered: the phase difference diffusion slows down with increasing noise intensity! Noise-induced ordering will be discussed in detail in Section 7.

5.2 Forced stochastic synchronization of the Schmitt trigger

When studying the synchronizing action of an external periodic signal on stochastic bistable systems, the global dynamics of transitions between metastable states is of much interest. Hence, in order to explore the effect of synchronization it is suitable to use an ideal bistable system — the Schmitt trigger [10, 102].

Experimental investigations of the mean switching frequency for the Schmitt trigger were performed in Ref. [90]. Noise with a cutoff frequency $f_c = 100$ kHz and a periodic signal with frequency $f_0 = 100$ Hz were applied to the Schmitt trigger with a threshold voltage $\Delta U = 150$ mV.

In accordance with the output signal, which represents a telegraph process and is registered by a computer, we

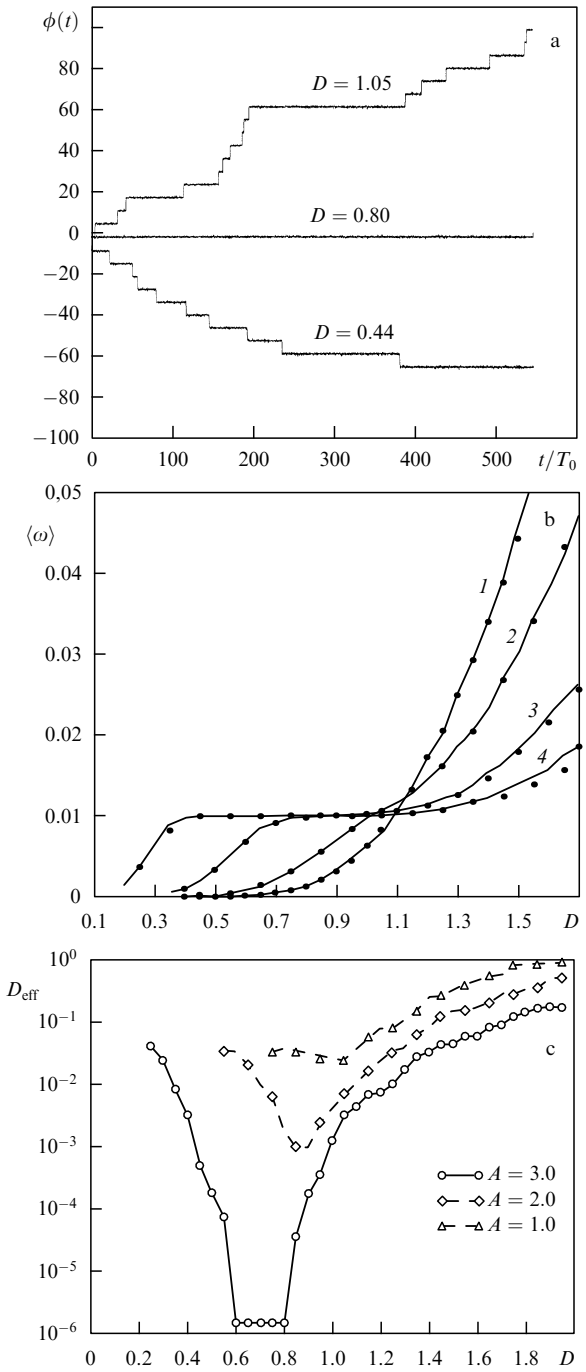

Figure 6. (a) Instantaneous phase difference ϕ against time for indicated values of the noise intensity; other parameters are: $A = 3$, $\alpha = 5$, $\beta = 1$, $\Omega_0 = 0.01$; (b) the mean frequency (5.10) (solid line) and the mean switching frequency (5.14) (symbols •) versus noise intensity for different values of the driving amplitude: *1* — $A = 0$, *2* — $A = 1$, *3* — $A = 2$, and *4* — $A = 3$; (c) the effective diffusion coefficient as a function of the noise intensity for indicated values of the driving amplitude; other parameters are: $\alpha = 5$, $\beta = 1$, $\Omega_0 = 0.01$.

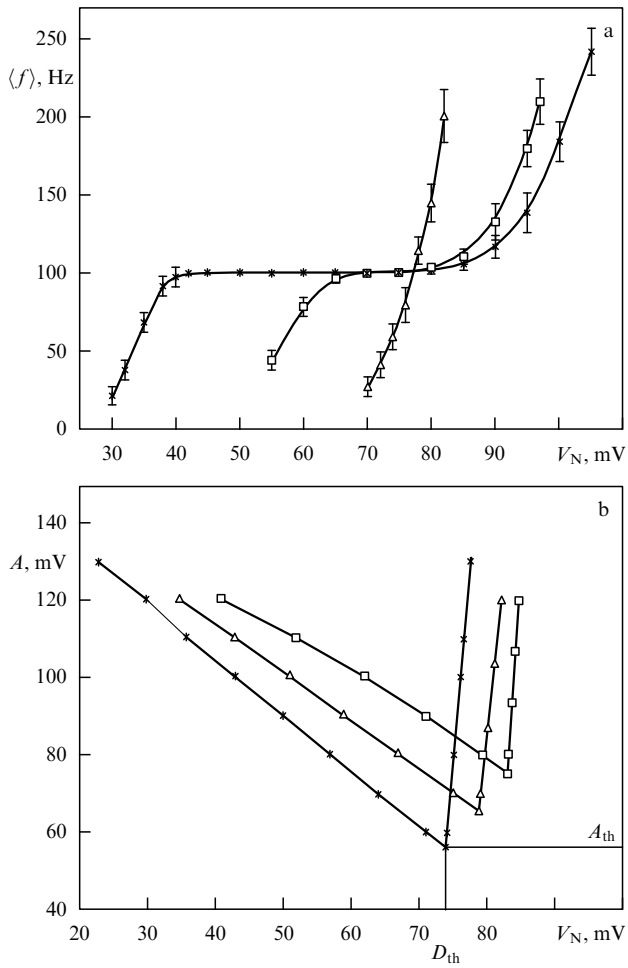

Figure 7. (a) Mean frequency $\langle f\rangle$ of the output signal of the Schmitt trigger (experiment) as a function of the noise amplitude V_{N} for different signal amplitudes: $A = 0$ mV (△), $A = 60$ mV (□), $A = 100$ mV (⋆); (b) synchronization regions for the Schmitt trigger for different signal frequencies: $f_0 = 100$ Hz (⋆), $f_0 = 250$ Hz (△), and $f_0 = 500$ Hz (□).

measured the mean frequency using definition (5.14). The results of measurements are shown in Fig.7. For a weak signal, the dependence of the mean frequency on the noise intensity obeys Kramers law. With increasing signal amplitude, the dependence is qualitatively different: there is a range of noise intensities where the mean frequency practically does not change with increasing noise and, within the limits of experimental accuracy, remains equal to the signal frequency. The effect of mean switching frequency locking is observed (see Fig. 7a) [90].

Repeating the measurements of the mean frequency for different values of the amplitude and phase of the signal one may obtain synchronization regions on the parameter plane 'noise intensity – amplitude of periodic force', where the mean frequency matches the signal frequency. Synchronization regions resembling Arnold's tongues are shown in Fig. 7b. As seen from the picture, there is a threshold amplitude A_{th} from which the effect of mean frequency locking is observed. When the threshold is achieved, the periodic signal starts to effectively control the stochastic dynamics of switchings. With increasing signal frequency, the synchronization is adversely affected: the synchronization regions contract, and the threshold value of the signal amplitude increases (see Fig. 7b).

Figure 8 illustrates the residence-time probability density $P(t)$ of the trigger in one of the metastable states for different noise intensities. For a weak noise, $P(t)$ exhibits peaks centred at odd multiples of the half signal period. Inside the synchronization region the mean residence time in one of the states coincides with the half period and the residence-time probability density possesses a single well-marked peak at

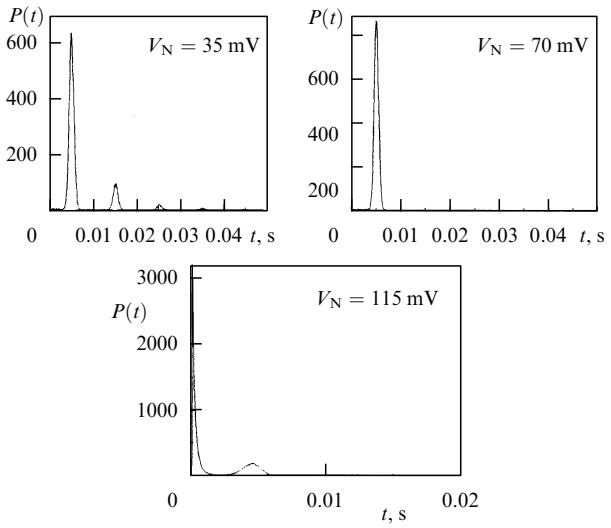

Figure 8. Residence-time probability density for the Schmitt trigger in one of the states. Signal amplitude $A = 100$ mV, and signal frequency $f_0 = 100$ Hz.

$t = T_0/2$. For a high noise ($V_N = 115$ mV), beyond the synchronization region, the mean time for switchings is much less than the half period. In one period the system switches repeatedly from one state to another, and a peak corresponding to short switching times appears. The peak centred at the half signal period is smeared and coherence of the output signal is destroyed.

The Schmitt trigger is modelled by the equation [28]

$$y(t + \Delta t) = \operatorname{sgn}\left[Ky(t) - \xi(t) - A\sin \Omega t\right], \qquad (5.15)$$

where $K = 0.2$ characterizes the operating threshold of the trigger, $\xi(t)$ is the exponentially correlated Gaussian noise with correlation time $\tau_c = 10^{-2}$, and the intensity D is governed by an Ornstein – Uhlenbeck process

$$\dot{\xi} = -\frac{1}{\tau_c}\,\xi + D\sqrt{\frac{2}{\tau_c}}\,w(t)\,, \qquad \left\langle w(t)w(t+\tau)\right\rangle = \delta(\tau)\,. \quad (5.16)$$

The dependences of the mean switching frequency of the trigger versus noise intensity obtained by numerical simulation of Eqns (5.15), (5.16) for different values of the modulation amplitude have completely verified the experimental results shown in Fig. 7a. The dynamics of the phase difference resulting from definition (5.13) seemed to be qualitatively equivalent to the case of the bistable oscillator (see Fig. 6a). This confirmed the effect of trigger switching phase locking by external signal at an optimal value of the noise intensity.

From the findings presented above it follows that an external periodic signal of sufficient amplitude synchronizes the stochastic dynamics of the switching events. Note two important moments. Although the signal amplitude is beyond the limits of applicability of the linear response theory, it remains so small that in the absence of noise the system cannot be switched. Therefore, noise is a necessary part of the phenomenon being considered. This phenomenon is accompanied by instantaneous phase and mean frequency locking. What is more, in the synchronization regime the level of phase fluctuations is substantially reduced, i.e. the effective diffusion coefficient is minimized.

5.3 Mutual stochastic synchronization of coupled bistable systems

Now we consider the simple case of two symmetrically coupled overdamped bistable oscillators described by the SDE [94, 103]

$$\dot{x} = \alpha x - x^3 + \gamma(y - x) + \sqrt{2D}\,\xi_1(t)\,,$$
$$\dot{y} = (\alpha + \Delta)y - y^3 + \gamma(x - y) + \sqrt{2D}\,\xi_2(t)\,. \qquad (5.17)$$

In the last set of equations the parameter α determines the Kramers frequency of the first subsystem without coupling, Δ is the parameter of detuning of the second system with respect to the first, and γ is the coupling coefficient. The white noise sources $\xi_1(t)$ and $\xi_2(t)$ are assumed to be statistically independent: $\left\langle \xi_i(t)\xi_j(t+\tau)\right\rangle = \delta_{i,j}\delta(\tau)$. The latter means that for $\gamma = 0$ the stochastic processes $x(t)$ and $y(t)$ in the subsystems will also be statistically independent. We also assume the intensities of uncorrelated noises to be identical: $D_1 = D_2 = D$. A detailed bifurcation analysis of this system was made in Ref. [94].

Since individual subsystems are bistable, we assume the processes $x(t)$ and $y(t)$ to be synchronized if the transitions between metastable states in the subsystems occur at the same time moments. The value of detuning parameter $\Delta = -0.5$ represents faster motion in the second subsystem $y(t)$. It has been established experimentally that for weak coupling the processes in the subsystems are nonsynchronized. By increasing the coupling coefficient the process in the second subsystem becomes slower, and for a sufficient value of γ the processes in the subsystems become coherent [94, 103].

To quantify the synchronization process we use the coherence function defined by the expression

$$\Gamma^2(\omega) = \frac{\left|G_{xy}(\omega)\right|^2}{G_{xx}(\omega)G_{yy}(\omega)}\,, \qquad (5.18)$$

where $G_{xy}(\omega)$ is the mutual spectral density of the processes $x(t)$, $y(t)$, while $G_{xx}(\omega)$ and $G_{yy}(\omega)$ are the power spectra of $x(t)$ and $y(t)$, respectively.

The coherence function obtained numerically from the simulation of SDE (5.17) is shown in Fig. 9a for different values of the coupling coefficient. The stochastic processes $x(t)$, $y(t)$ are coherent in the low-frequency range corresponding to the Kramers frequencies of the subsystems.

Let us explore the evolution of the characteristic time scales of the subsystems as one varies the coupling coefficient. For $\gamma = 0$, the natural time scales of the subsystems are represented by the Kramers rates (frequencies) r_x, r_y of escape from a metastable state:

$$r_x = \frac{\sqrt{2}\,\alpha}{\pi}\exp\left(-\frac{\alpha^2}{4D}\right),$$
$$r_y = \frac{\sqrt{2}(\alpha + \Delta)}{\pi}\exp\left[-\frac{(\alpha + \Delta)^2}{4D}\right]. \qquad (5.19)$$

The dependence of the mean switching frequencies on γ is shown in Fig. 9b. With increasing coupling strength the mean frequencies of the partial subsystems come closer together. The coherence function characterizes only a degree of linear dependence and contains no information about the phases of the processes. The instantaneous phase of the processes in the subsystems can be introduced on the basis of the switching times t_i^x, t_j^y in a similar manner as was done in the previous section. Numerical simulation of the dynamics of instanta-

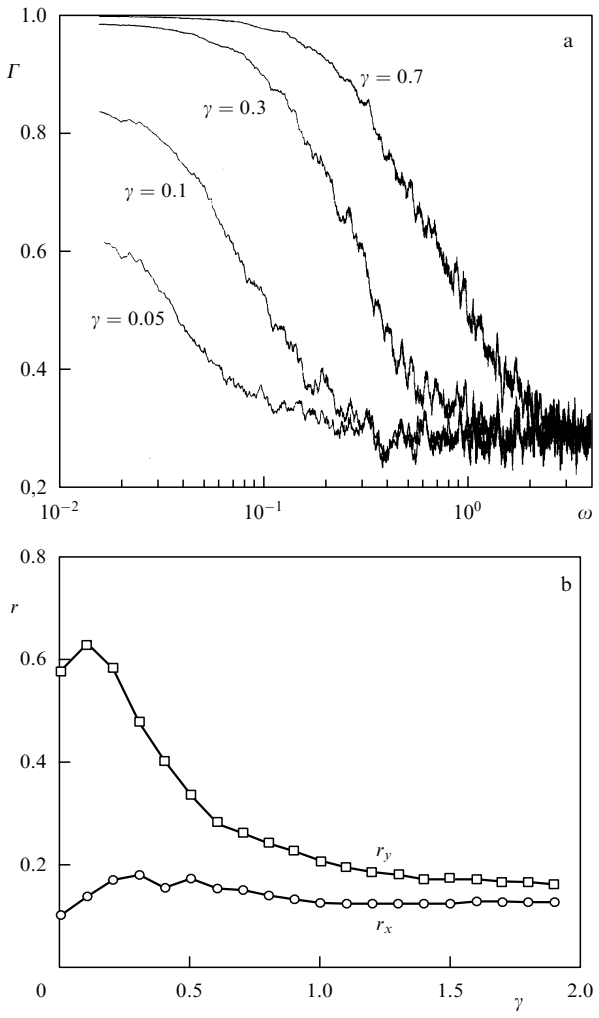

Figure 9. (a) Coherence function $\Gamma(\omega)$ for the system governed by Eqn (5.17) for different values of the coupling coefficient, and (b) the mean switching frequencies $r_{x,y}$ as functions of the coupling coefficient for parameters $\alpha = 1.0$, $\Delta = -0.5$, and $D = 0.1$.

neous phase difference $\phi(t) = \Theta_x(t) - \Theta_y(t)$ has shown the effect of phase synchronization for $\gamma > 1$: the phase difference remains constant over long time intervals.

5.4 Forced and mutual synchronization of switchings in chaotic systems

As has been already noted, the effect of deterministic SR is realized in chaotic systems in the regimes of 'chaos – chaos' intermittency. In this case the mean frequency of irregular switching events is governed by a control parameter (see Section 4.2).

If these phenomena are united by a deep physical generality, then in chaotic systems with strong interactions one must observe the effect of synchronization of switchings which is qualitatively equivalent to that described above for stochastic bistable systems. And this is actually so. For illustrative purposes we shall discuss forced and mutual synchronization of switching events in systems with deterministic chaotic dynamics.

Forced synchronization. Let us turn again to map (4.12) and consider the regime of 'chaos – chaos' intermittency for $a > a_{cr} = 2.839\ldots$ Let us study the system's dynamics in the absence of external noise for a large enough amplitude A of the external periodic force. Then the switching process is principally nonlinear and its statistics depends essentially on the parameters a, A and ω. Using the two-state method we evaluate the evolution of the residence-time probability density $p(\tau)$ on a single attractor as parameter a is varied. The results are shown in Fig. 10 and qualitatively follow the data presented in Fig. 8. At a certain value $a = 8.34$ the distribution possesses a single Gaussian-like peak with a maximum at $\tau = 0.5$. This means that the mean frequency of switchings between chaotic attractors coincides with the external force frequency.

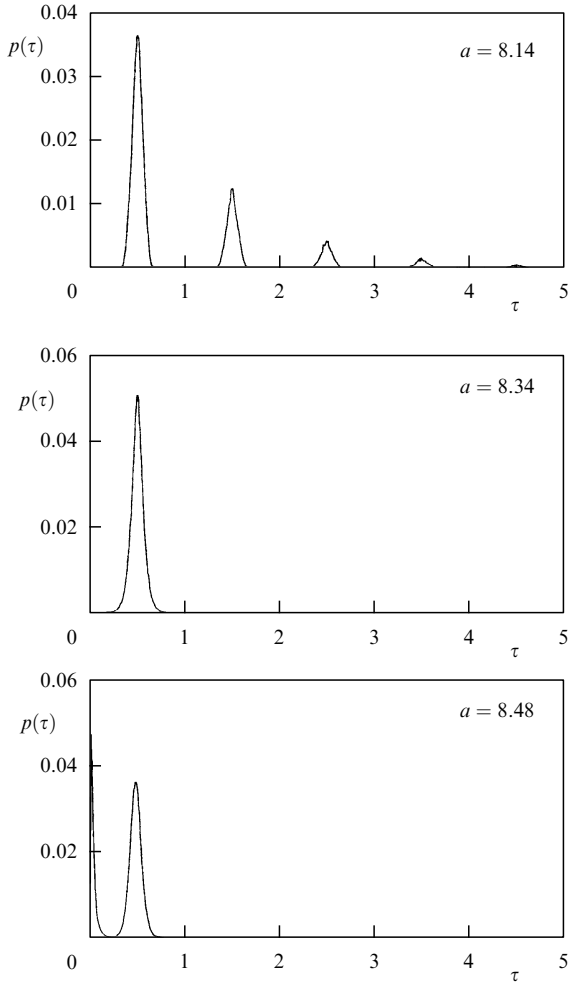

Figure 10. Evolution of the residence-time probability density as the control parameter a is varied.

The effect of mean switching frequency locking by the external signal is illustrated in Fig. 11a for different values of parameter a. With increasing signal amplitude, the synchronization region expands as expected. As seen from Fig. 11b, this region is a typical synchronization zone as for the Schmitt trigger (Fig. 7b) and also demonstrates a threshold character of synchronization. Hence, the effect of forced synchronization of the switching frequency in a deterministic chaotic system is confidently observed and proves to be equivalent to the effect of noise-induced stochastic synchronization, described in Sections 5.1 and 5.2.

The effect of mean switching frequency locking is universal and manifests itself in a wide class of dynamical

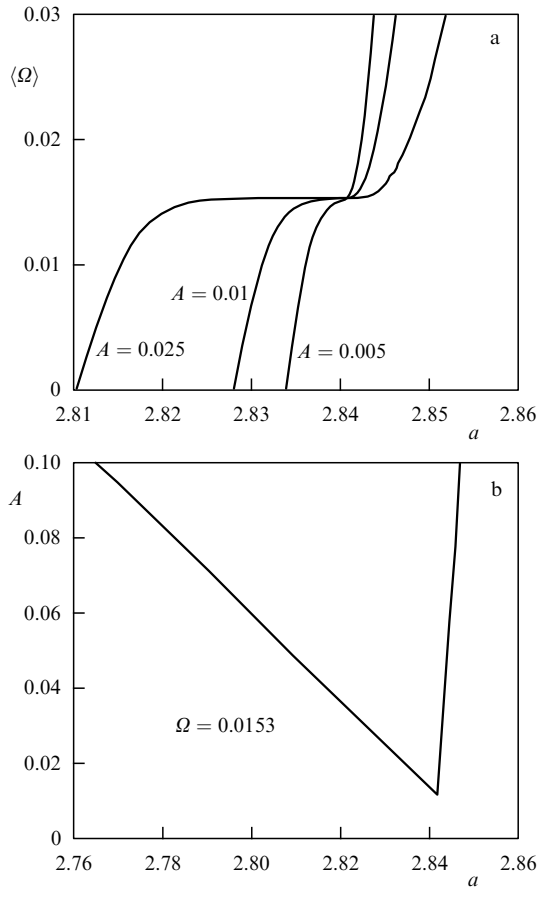

Figure 11. (a) Mean switching frequency vs. parameter a for different values of the signal amplitude, and (b) the synchronization region of the switching frequency for map (4.12).

systems with intermittency. As an example we shall study the nonlinear Chua system realizing the regime of dynamical intermittency [35, 83]. Chua's circuit is described by a set of equations

$$\begin{aligned} \dot{x} &= \alpha\big[y - h(x)\big]\,, \\ \dot{y} &= x - y + z\,, \\ \dot{z} &= -\beta y + F(t)\,, \end{aligned} \tag{5.20}$$

where $h(x) = m_1 x + 0.5(m_0 - m_1)\big(|x+1| - |x-1|\big)$ is the piecewise-linear characteristic of the system with fixed parameters $m_0 = -1/7$, $m_1 = 2/7$, and $F(t) = a\cos\omega_c t$ is the external periodic force.

As was shown in Ref. [83], the switching process in the chaotic bistable system (5.20) has a purely dynamical nature. We again apply the two-state approach. Let parameter β be fixed, namely, $\beta = 14.286$. The dynamics of the system depends on α as well as on the amplitude a and frequency ω_c of the external signal. Without driving signal ($a = 0$) an intermittency is realized for $\alpha \approx 8.8$. With increasing α, when $\alpha > 8.8$, the mean switching frequency (the analogue of the Kramers frequency) monotonically increases. We choose the amplitude value $a = 0.1$ when the system response to the external force is, in principle, nonlinear.

The results of numerical calculations of the return-time probability density $p(\tau)$ for different values of α have shown a surprising similarity to the data obtained for the Schmitt trigger and displayed in Fig. 8. For a certain value $\alpha = 8.8325$, the probability density $p(\tau)$ has a single Gaussian-like peak near $\tau = 1$. This means that the mean switching frequency coincides with the external force frequency. The effect of forced synchronization is registered. This manifests itself in the mean switching frequency locking by the periodic signal. The numerical data are presented in Fig. 12 and illustrate synchronization regions on the parameter plane 'external signal amplitude – control parameter α'. These regions are qualitatively similar to Arnold's tongues as in the case of the Schmitt trigger (Fig. 7b). The only difference is that, as the signal frequency increases, the threshold of the synchronization process practically does not change and the width of the synchronization regions is increased. These differences are caused by the nonlinear properties of the system (5.20) and do not relate to the nature of the observed phenomenon. More detailed calculations demonstrate that the effect of mean switching frequency synchronization in systems (4.12) and (5.20) corresponds to the effect of phase synchronization, which is completely equivalent to the cases of the Schmitt trigger and the overdamped oscillator considered above.

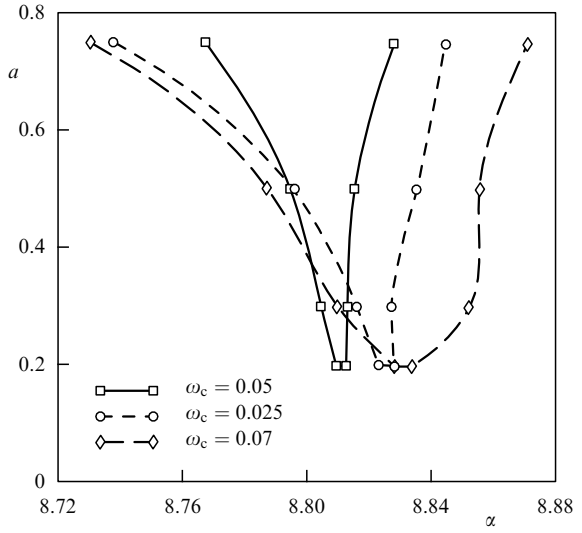

Figure 12. Synchronization regions for Chua's system.

Mutual synchronization. As an example of mutual synchronization of switching events, we shall examine the dynamics of two coupled Lorenz models [104]

$$\begin{aligned} \dot{x_1} &= \sigma(y_1 - x - 1) + \gamma(x_2 - x_1)\,, \\ \dot{y_1} &= r_1 x_1 - x_1 z_1 - y_1\,, \\ \dot{z_1} &= x_1 y_1 - z_1 b\,, \\ \dot{x_2} &= \sigma(y_2 - x_2) + \gamma(x_1 - x_2)\,, \\ \dot{y_2} &= r_2 x - 2 - x_2 z_2 - y_2\,, \\ \dot{z_2} &= x_2 y_2 - z_2 b\,. \end{aligned} \tag{5.21}$$

We choose the parameters to be: $\sigma = 10$, $r_1 = 28.8$, $r_2 = 28$, and $b = 8/3$, when the Lorenz attractor is realized in each of the subsystems [84, 87]. The Lorenz attractor in an individual system may be treated as a generalized bistable oscillator where irregular switching events occur with a mean frequency controlled by the parameter γ. The introduction of coupling ($\gamma > 0$) must cause changes of the mean switching frequencies in each of the subsystems and lead to the effect of mutual synchronization of switchings.

As calculations carried out in the two-state approximation have shown, the mean switching frequencies $\langle f_1 \rangle$ and $\langle f_2 \rangle$ practically coincide for a coupling coefficient $\gamma > 5$. Moreover, numerical simulation of the dynamics of the instantaneous phase difference between $x_1(t)$ and $x_2(t)$ processes has confirmed the effect of mutual synchronization: for $\gamma > 5$, the phase difference approaches zero at times significantly exceeding the mean switching time. Therefore, the effect of mutual synchronization takes place for strong coupling between two chaotic bistable oscillators.

6. Stochastic resonance and synchronization of ensembles of stochastic resonators

The effect of SR can be significantly enhanced if an array of coupled bistable systems is taken instead of a single one [105 – 108]. It has been found out that at optimal values of the noise intensity and the coupling coefficient the SNR in an array attains its maximal level, demonstrating an array-enhanced SR effect [103, 109]. We consider first the case of extremely weak coupling when the interaction between individual stochastic resonators might be neglected.

A model under study contains N subsystems, each demonstrating SR. Partial subsystem SR_k possesses an internal noise $\xi_k(t)$. In addition, the internal noises in the subsystems are statistically independent. Each resonator is subjected to the same input signal $s(t)$ which may be aperiodic. The outputs of the elements are converged onto a summing centre giving a collective response $x_M(t)$:

$$x_M(t) = \frac{1}{N} \sum_{k=1}^{N} x_k(t) \,. \tag{6.1}$$

This model is widely used in practice as the simplest method for increasing the signal-to-noise ratio [110]. When the number of elements in the array is sufficiently large ($N \gg 1$), the internal noises at the collective output disappear due to averaging and the SNR increases proportionably to the number of elements. This model is truly nontrivial because each element is treated as a stochastic resonator. Hence, besides enhancement of the SNR, it is also possible to amplify significantly the signal. Synchronization of an ensemble by an external signal is also of great interest. We note that this model has important biological applications relating to, for example, a simple network of sensory neurons [111] and a model of ion channels [112, 113]. A similar model, where self-excited systems were used as individual elements, has been studied in Ref. [114]. Using this model, the important effect of 'stochastic resonance without tuning' was established in Ref. [115]: on increasing the number of elements in the array the dependence of the SNR on the noise intensity disappears beyond a certain small threshold value.

6.1 Linear response theory for arrays of stochastic resonators

In the case of a weak signal $s(t)$ the statistical properties of the response of a single stochastic system can be calculated via LRT. The problem is to compute the spectral characteristics of the collective response $x_M(t)$ [68].

Denote the spectral density at the output of the kth element by $G_{kk}(\omega)$, the cross spectral density of the kth and mth elements by $G_{km}(\omega)$ and the spectral density at the summing output by $G_{MM}(\omega)$. The spectral density $G_{MM}(\omega)$ is derived immediately from (6.1) as follows

$$G_{MM}(\omega) = \frac{1}{N^2} \left[\sum_{k=1}^{N} G_{kk}(\omega) + \sum_{k=1}^{N} \sum_{\substack{m=1 \\ k \neq m}}^{N} G_{km}(\omega) \right] . \tag{6.2}$$

In the absence of the signal $G_{km}(\omega) = 0$ by virtue of the statistical independence of the internal noises in the elements. Each element of the array has a known susceptibility $\chi_k(\omega, D)$, where D is the intensity of internal noise. For the spectral density at the output of the kth element we have

$$G_{kk}(\omega) \approx G_{kk}^{(0)}(\omega, D) + \left|\chi_k(\omega, D)\right|^2 G_{ss}(\omega) \,, \tag{6.3}$$

where $G_{kk}^{(0)}(\omega, D)$ is the spectral density of the kth element without a signal, and $G_{ss}(\omega)$ is the spectral density of the input signal. The cross spectral density $G_{km}(\omega)$ is determined as [68]

$$G_{km}(\omega) = \chi_k^*(\omega, D)\, \chi_m(\omega, D)\, G_{ss}(\omega) \,, \tag{6.4}$$

where the symbol $*$ denotes complex conjugation. In the absence of the signal $G_{km}(\omega) = 0$. Substituting (6.3), (6.4) into (6.2) we obtain the spectral density of the collective output

$$G_{MM}(\omega) = \frac{1}{N^2} \sum_{k=1}^{N} G_{kk}^{(0)}(\omega, D) + \frac{G_{ss}(\omega)}{N^2} \sum_{k=1}^{N} \sum_{m=1}^{N} \chi_k^*(\omega, D) \chi_m(\omega, D) \,. \tag{6.5}$$

The cross spectral density of the collective output and the input signal $G_{sM}(\omega)$ reads as

$$G_{sM}(\omega) = \frac{G_{ss}(\omega)}{N} \sum_{k=1}^{N} \chi_k(\omega, D) \,. \tag{6.6}$$

The relations obtained allow one to determine all the necessary SR measures, in particular, the coherence function and the SNR. In order to simplify our analysis we consider an array of identical elements with susceptibility $\chi(\omega, D) \equiv \chi_k(\omega, D)$ and unperturbed spectral density $G_{xx}^{(0)}(\omega, D) \equiv G_{kk}^{(0)}(\omega, D)$. For this case we have the following expressions for the spectral densities

$$G_{MM}(\omega) = \frac{1}{N} G_{xx}^{(0)}(\omega, D) + \left|\chi(\omega, D)\right|^2 G_{ss}(\omega) \,, \tag{6.7}$$

$$G_{sM}(\omega, D) = \chi(\omega, D) G_{ss}(\omega) \,. \tag{6.8}$$

In the limit $N \to \infty$, the first item in Eqn (6.7), answering for the internal fluctuations in the elements of the array, disappears and the whole ensemble behaves as an equivalent *linear* system with the transfer function $\chi(\omega, D)$.

Let the input signal $s(t)$ be represented by a broadband Gaussian noise with zero mean and the spectral density $G_{ss}(\omega)$. We are interested in the coherence function $\Gamma(\omega)$ and the correlation coefficient C_1 linking the input with collective output:

$$\Gamma^2(\omega) = \frac{\left|G_{sM}(\omega)\right|^2}{G_{MM}(\omega)\, G_{ss}(\omega)} \,, \qquad C_1 = \frac{\langle x_M, s \rangle}{\sqrt{\langle s^2 \rangle \langle x_M^2 \rangle}} \,. \tag{6.9}$$

Inserting (6.7) and (6.8) to (6.9) we obtain the expression for the coherence function which is valid for weak signals:

$$\Gamma^2(\omega) = \frac{\left|\chi(\omega, D)\right|^2 G_{ss}(\omega)}{G_{xx}^{(0)}(\omega, D)/N + \left|\chi(\omega, D)\right|^2 G_{ss}(\omega)} \,. \tag{6.10}$$

When $N \to \infty$, the coherence function tends to 1, as it should for a linear system. As N becomes large, the dependence of the coherence function on D and on ω is no longer observed, as seen from formula (6.10). In other words, the output signal can be optimized for any internal noise intensity, beginning with a certain small value.

Let a weak input signal $s(t)$ be the sum of the periodic and noise components, i.e. $s(t) = n(t) + A \sin \Omega t$. The SNR at the input is fixed:

$$\mathrm{SNR}_{\mathrm{in}} = \frac{\pi A^2}{G_{nn}(\Omega)}\,, \tag{6.11}$$

where $G_{nn}(\omega)$ is the spectral density of the noisy component. The spectral density of the collective output will also consist of a noisy background and a δ-peak corresponding to the periodic part of the signal:

$$G_{MM}(\omega) = \frac{1}{N} G_{xx}^{(0)}(\omega, D) + \left|\chi(\omega, D)\right|^2 \times \left[G_{nn}(\omega) + \pi A^2 \delta(\omega - \Omega)\right]. \tag{6.12}$$

The SNR of the collective output, $\mathrm{SNR}_{\mathrm{out}}$, can easily be derived from the last expression. However, of much more interest is the ratio of the SNR at the output to the SNR at the input:

$$\eta = \frac{\mathrm{SNR}_{\mathrm{out}}}{\mathrm{SNR}_{\mathrm{in}}} = 1 - \frac{G_{xx}^{(0)}(\Omega, D)}{G_{xx}^{(0)}(\Omega, D) + N\left|\chi(\Omega, D)\right|^2 G_{nn}(\Omega)}\,. \tag{6.13}$$

This ratio is always less than 1, unless N tends to infinity, when the input and output SNRs coincide. Although, as follows from the analysis above, *the SNR at the output of the ensemble of stochastic resonators cannot be improved compared to the SNR at the input*, the periodic component of the signal can be significantly amplified by $\left|\chi(\Omega, D)\right|$ times.

Estimation of the number of elements necessary to achieve a given ratio η is of practical importance. This number can easily be found from Eqn (6.13):

$$N = \frac{G_{xx}^{(0)}(\Omega, D)}{\left|\chi(\Omega, D)\right|^2 G_{nn}(\Omega)} \frac{\eta}{1 - \eta}\,. \tag{6.14}$$

For an array of stochastic resonators the dependence $N(D)$ demonstrates a minimum at a certain optimal noise intensity. Therefore, at an optimal noise level the required value of the ratio η can be reached for a minimal number of elements in the array [68].

6.2 Synchronization of an ensemble of stochastic resonators by a weak periodic signal

In the limit of an infinite number of elements in the array and in the absence of external noise the collective response of the array to a weak periodic signal is a periodic function of time

$$x_M^{\infty}(t) = A\left|\chi(\Omega, D)\right| \cos(\Omega t + \psi)\,, \tag{6.15}$$

where ψ is the phase shift defined as

$$\psi = -\arctan \frac{\mathrm{Im}\,\chi(\Omega, D)}{\mathrm{Re}\,\chi(\Omega, D)}\,. \tag{6.16}$$

Situations when the number of elements is large but finite are of great interest. As examples from biology we can mention here populations of neuron-receptors [111] and arrays of ion channels in cell membranes [112, 113]. How much does the process at the collective output of the ensemble reflect the input signal? The previous sections have given an answer to this question only in terms of the averaged characteristics, such as the SNR and the coherence function.

As has been shown in Section 5, for a single stochastic resonator, synchronization of the output and input is possible only for a large enough amplitude of signal. In the case of an array of stochastic resonators the internal noise is reduced due to averaging at the summing output, so that it is possible to synchronize an array of stochastic resonators with an arbitrary weak periodic signal [116].

As an example we refer to an ensemble of Schmitt triggers

$$x_k(t + \Delta t) = \mathrm{sgn}\left[K x_k(t) - \xi_k(t) - \eta(t) - A \sin \Omega t\right], \tag{6.17}$$

where K is the operating threshold of the trigger, $\xi_k(t)$ is the internal noise in the kth element, and $\eta(t)$ is a weak external noise. In the numerical simulations $K = 0.2$, the internal noise was assumed to be Gaussian exponentially correlated noise with correlation time $\tau_c = 0.01$ and intensity D. The external noise was also Gaussian coloured noise with the same correlation time and intensity $Q = 0.03$. We chose the amplitude of the periodic signal $A = 0.03$ and the frequency $\Omega = 0.5$, at which the phenomenon of stochastic synchronization did not occur in a single element.

To quantify the synchronization of the collective output we use the notions of the mean frequency (5.10), (5.14) and the instantaneous phase (5.13). The mean frequency $\langle\omega\rangle$ is shown in Fig. 13a as a function of the internal noise intensity for different numbers of elements N in the array. For a single element $N = 1$, the dependence $\langle\omega\rangle(D)$ is exponential. However, with an increasing number of elements the exponential law is violated and for a large enough N ($N \geqslant 100$) the effect of $\langle\omega\rangle$-frequency locking takes place. This phenomenon is similar to synchronization of a single bistable resonator as the signal amplitude increases (see Fig. 6b and Fig. 7a). But in our case the signal amplitude is small and the synchronization can be achieved by virtue of the increase of the number of elements in the array.

The synchronization effect is also verified by calculations of the instantaneous phase difference of the collective output and the periodic signal. The results are shown in Fig. 13b. At an optimal internal noise intensity ($D \approx 0.06$), the phase difference remains constant for long time intervals. As has been already noted, the mean value of these time intervals can be estimated using the effective diffusion coefficient D_{eff} of the phase difference. As the calculations have shown, at an optimal noise intensity the effective diffusion coefficient is minimal. When the number of elements N in the array increases, the absolute value of the diffusion coefficient decreases, and the optimal intensity D of internal noise shifts to the range of smaller values.

The synchronization phenomenon described above is observed for any elements demonstrating SR as one varies the internal noise, including elements which can be represented by neuron models.

6.3 Stochastic resonance in a chain with finite coupling between elements

When stochastic resonators are coupled, we may further optimize the amplification properties of the system as the coupling coefficient is varied [103, 105, 106, 108]. In this

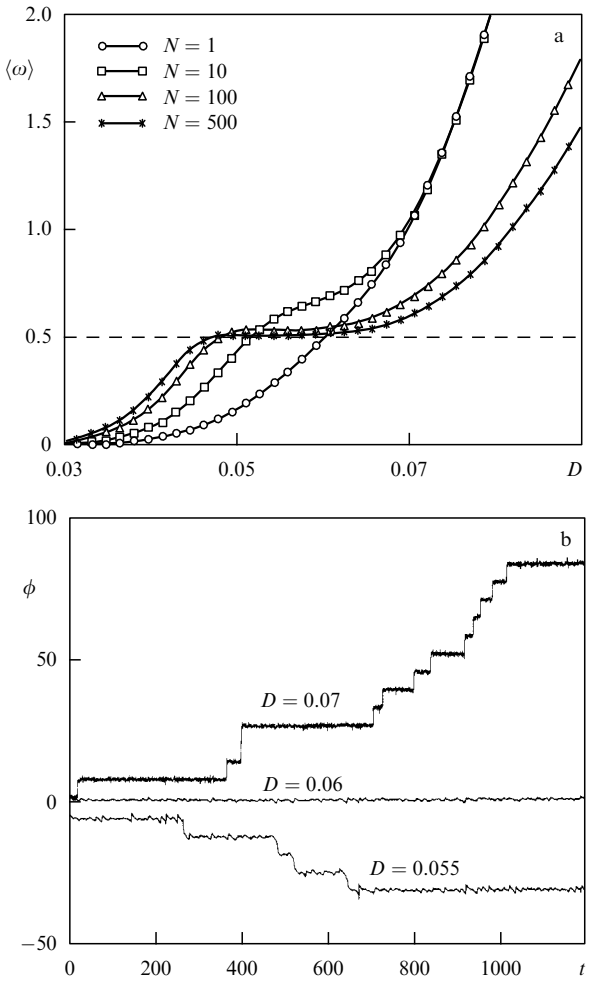

Figure 13. (a) Mean frequency $\langle\omega\rangle$ of the collective output for the ensemble of Schmitt triggers as a function of the internal noise intensity D for different numbers of elements N in the ensemble, and (b) time series of the phase difference between the collective output and the periodic input for an ensemble of 100 Schmitt triggers for different values of the internal noise intensity.

section we consider a chain of coupled systems with two discrete states, namely, a chain of coupled spins. The system is modulated by a periodic external (magnetic) field. Each spin is able to flop due to thermal noise. The elements are coupled via magnetic interaction. This model is one of the best studied systems of coupled elements and goes back to R Glauber (1963) [117]. In this connection the stochastic dynamics of a chain of coupled spins has come to be known as Glauber's dynamics.

Glauber's dynamics was used for finding SR in ferromagnetic systems. In this case the flip-flop rate α was constant and temperature-independent, so that SR takes place only when there is an interaction between spins. Numerical experiments on a two-dimensional Ising model performed in Ref. [20] have confirmed the existence of SR. The authors of Ref. [118] found an optimal coupling for a given temperature T in a spin chain with a constant flip-flop rate α.

We make use of the idea that a chain of coupled spins can be considered as the simplest prototype of coupled bistable stochastic resonators [109]. Notice that the flip-flop rate of a single spin in Glauber's model is assumed to be temperature-dependent. In addition to Glauber approximation we suggest that the transition rate α between states $\sigma = +1$ and $\sigma = -1$ of an individual uncoupled spin obeys an Arrhenius-type law [27]

$$\alpha = \alpha_0 \exp\left(-\frac{1}{T}\right), \tag{6.18}$$

where it is supposed that $\alpha_0 = 1$.

A similar assumption about the temperature dependence, i.e. on noise intensity, was fundamental in the two-state theory [28] considered above for a single bistable system (see Section 2.1), where an element with two states, say $\sigma = \pm 1$, and stochastic switchings between them, described by the master equation

$$\dot{p}(\sigma) = -p(\sigma)W(\sigma, t) + p(-\sigma)W(-\sigma, t), \tag{6.19}$$

were considered. In Eqn (6.19), $p(\sigma)$ is the probability of residing element in state σ at time t, and $W(\sigma, t)$ denotes the transition probability per unit time for a flip-flop $\sigma \to -\sigma$. In the presence of a weak slowly varying periodic field the transition rates can be written as

$$W(\sigma, t) = \frac{\alpha}{2}\left(1 - \sigma\beta\cos(\Omega t + \phi)\right), \tag{6.20}$$

and in the limit $t_0 \to -\infty$ we can derive an expression for the SNR. The signal amplitude A enters the rates via $\beta = A/T$. In the continuous-state bistable systems such transition rates can be gained with sufficiently small amplitudes in the framework of the adiabatic approach.

To extend the two-state theory to coupled systems we consider a chain of infinitely many spins. We examine one or a few spins embedded in this chain. The state of the chain, which is specified by the sequence $\bar{\sigma} = (\ldots, \sigma_k - 1, \sigma_k, \sigma_k + 1, \ldots)$ $(\sigma_k = \pm 1)$, is occupied with probability $p(\bar{\sigma})$. The transition rates for a single element retain the form used in the two-state theory. In addition, the transition rates in coupled systems should depend on the states of the elements to the left and to the right with relation to a chosen element. Following Glauber consideration we write down the transition rates in the form

$$W_i(\sigma_i) = \frac{\alpha}{2}\left[1 - \sigma_i \frac{\gamma}{2}(\sigma_{i-1} + \sigma_{i+1})\right]. \tag{6.21}$$

For a positive γ, formula (6.21) gives enhanced rates for a parallel ordering of the spins. According to Glauber, the transition rates lead to a stationary state of the system characterized by the equilibrium distribution (the Ising model)

$$p_{\mathrm{eq}}(\bar{\sigma}) = Z^{-1}\exp\left(-\frac{1}{T}\mathcal{H}\right) = Z^{-1}\exp\left(\frac{1}{T}\sum_i J\sigma_i\sigma_{i+1}\right), \tag{6.22}$$

where Z^{-1} is the normalization constant. For lack of external action, the principle of detailed balance implies that

$$W_i(\sigma_i)p_{\mathrm{eq}}(\ldots, \sigma_{i-1}, \sigma_i, \sigma_{i+1}, \ldots) = W_i(-\sigma_i)p_{\mathrm{eq}}(\ldots, \sigma_{i-1}, -\sigma_i, \sigma_{i+1}, \ldots), \tag{6.23}$$

which is satisfied by choosing

$$\gamma = \tanh\frac{2J}{T}. \tag{6.24}$$

Here the parameter J has meaning of a coupling coefficient.

Taking into account the spin interaction of the type given by Eqn (6.21) and a periodic modulation by an external magnetic field as in (6.20) we obtain the transition rates in the following form:

$$W_i(\sigma_i) = \frac{\alpha}{2}\Big\{1 - \frac{\gamma}{2}\,\sigma_i(\sigma_{i-1} + \sigma_{i+1}) - \beta\Big[\sigma_i - \frac{\gamma}{2}(\sigma_{i-1} + \sigma_{i+1})\Big]\cos(\Omega t + \phi)\Big\}. \quad (6.25)$$

One can easily check that insertion of a Hamiltonian

$$\mathcal{H} = -\mu\sum_i H(t)\sigma_i - J\sum_i \sigma_i\sigma_{i+1} \quad (6.26)$$

into the equilibrium distribution (6.22) leads in the adiabatic limit under detailed balance conditions (6.23) to $\beta = \tanh(\mu A/T)$ or $\beta \approx \mu A/T$ for small amplitudes A. For simplicity, we set $\mu = 1$. The evolution of probabilities $p(\bar{\sigma})$ is governed by the master equation

$$\dot{p}(\bar{\sigma}) = \sum_k W_k(-\sigma_k)\,p(\ldots, \sigma_{k-1}, -\sigma_k, \sigma_{k+1}, \ldots) - \sum_k W_k(\sigma_k)p(\ldots, \sigma_{k-1}, \sigma_k, \sigma_{k+1}, \ldots)\,. \quad (6.27)$$

Apart from the harmonic external force and the temperature-dependent rates (6.18) this is Glauber's dynamics of the Ising model in the weak-field limit [117].

Note that the suggested model is an expansion of the two-state model [28] to the case of a chain of coupled bistable elements.

From Eqn (6.27) it follows that $\mathrm{d}\langle\sigma_k\rangle/\mathrm{d}t = -2\langle\sigma_k W_k(\sigma_k)\rangle$. This allows us to derive the set of differential equations for the first moments $\langle\sigma_k(t)\rangle$:

$$\frac{\mathrm{d}\langle\sigma_k\rangle}{\mathrm{d}t} = -\alpha\langle\sigma_k\rangle + \alpha\beta\cos(\Omega t + \phi) + \frac{\alpha\gamma}{2}\big(\langle\sigma_{k-1}\rangle + \langle\sigma_{k+1}\rangle\big) - \frac{\alpha\beta\gamma}{2}(r_{k-1,k} + r_{k,k+1})\cos(\Omega t + \phi)\,, \quad (6.28)$$

where $r_{i,j}(t) = \langle\sigma_i(t)\sigma_j(t)\rangle$. The system (6.28) is unclosed because it contains cross correlators $r_{i,j}(t)$. The closure of the system can be obtained by linearizing over parameter β. In this case the correlators $r_{i,j}$ may be taken from the unperturbed model ($\beta = 0$). The stationary values of the correlators are $r_{i,j} = \eta^{|i-j|}$, where $\eta = \gamma^{-1}\big(1 - \sqrt{1-\gamma^2}\big) = \tanh(J/T)$ [117].

We can further simplify the closed system being defined. Since all spins are uniformly forced by a magnetic field and their number is infinite, then, as the initial distribution of spins is forgotten, it is impossible to distinguish any single spin from the others. In other words, all spins will have the same statistics and the spin indices in Eqn (6.28) may be dropped. Taking into consideration the assumption that β is small, we arrive at the simplified equation for the mean state variable:

$$\frac{\mathrm{d}\langle\sigma\rangle}{\mathrm{d}t} = -\alpha(1-\gamma)\langle\sigma\rangle + \alpha\beta\sqrt{1-\gamma^2}\,\cos(\Omega t + \phi)\,. \quad (6.29)$$

Evidently, the dynamics of $\langle\sigma\rangle$ is identical to that of the mean state variable of an uncoupled spin with a renormalized relaxation rate $\alpha(1-\gamma)$ and modulation amplitude $\alpha\beta\sqrt{1-\gamma^2}$. In the limit of small external force amplitudes $\beta \approx A/T$ and the asymptotic solution of Eqn (6.29) reads as

$$\langle\sigma(t)\rangle = q\cos(\Omega t + \phi + \psi)\,,$$
$$q = q_{\mathrm{s}}\left[1 + \frac{\Omega^2}{\alpha^2(1-\gamma)^2}\right]^{-1/2}, \qquad \tan\psi = -\frac{\Omega}{\alpha(1-\gamma)}\,, \quad (6.30)$$

where q_{s} is the response to a static signal ($\Omega = 0$):

$$q_{\mathrm{s}} = \frac{A}{T}\sqrt{\frac{1+\gamma}{1-\gamma}} = \frac{A}{T}\exp\left(\frac{2J}{T}\right). \quad (6.31)$$

Since the magnitude of the static response should not exceed unity ($q_{\mathrm{s}} = 1$), expression (6.31) imposes additional restrictions on the parameters of the system for which the suggested approximations retain their validity:

$$A \ll \min\left[T, T\exp\left(-\frac{2J}{T}\right)\right]. \quad (6.32)$$

The spectral density of the spin state is determined from the correlation function $\big\langle\sigma_k(t)\sigma_k(t+\tau)\big\rangle$, where the periodic non-stationarity is removed by additional averaging $\langle\ \rangle_\phi$ over a uniformly distributed initial phase of the signal. Introducing the correlation function

$$c_{kk}(t,\tau) = \big\langle\big[\sigma_k(t) - q_k(t)\big]\big[\sigma_k(t+\tau) - q_k(t+\tau)\big]\big\rangle$$

we find

$$\big\langle\big\langle\sigma_k(t)\sigma_k(t+\tau)\big\rangle\big\rangle_\phi = \big\langle c_{kk}(t,\tau)\big\rangle_\phi + \frac{q^2}{2}\cos\Omega\tau\,. \quad (6.33)$$

The second term on the right of Eqn (6.33) gives a δ-function with πq^2 weight at the signal frequency. The first term forms the continuous part of the spectrum. For our purposes it is sufficient to approximate the continuous part of the spectrum by the spectral density of the unperturbed system. In this case the stationary correlation function $c(\tau)$ does not depend on the initial phase of the signal or on the spin index. In accordance with Glauber's theory $c(\tau)$ is defined as

$$c(\tau) = \exp\big(-\alpha|\tau|\big)\sum_{n=-\infty}^{+\infty}\eta^{|n|}I_n\big(\alpha\gamma|\tau|\big)\,, \quad (6.34)$$

where $I_n\big(\alpha\gamma|\tau|\big)$ is the modified Bessel functions. The spectral density reads as [119]

$$G(\omega) = 4\,\mathrm{Re}\,\frac{1+\eta s_2}{s_1(1-\eta s_2)}\,, \qquad \omega > 0\,, \quad (6.35)$$

where $s_1 = \sqrt{(\alpha+\mathrm{i}\omega)^2 - (\alpha\gamma)^2}$ and $s_2 = \alpha\gamma(\alpha + \mathrm{i}\omega + s_1)^{-1}$.

Now we can obtain analytic expressions for the SPA and the SNR. Both measures are calculated for a single spin embedded in a chain of infinite length. The SPA, $\rho = (q/A)^2$, is given by the explicit expression,

$$\rho = \frac{1}{T^2}\exp\left(\frac{4J}{T}\right)\left\{1 + \left[\frac{\Omega\exp(1/T)}{1 - \tanh(2J/T)}\right]^2\right\}^{-1}. \quad (6.36)$$

The SNR normalized on the square of the signal amplitude is

$$\mathrm{SNR} = \frac{\pi q^2}{A^2 G(\Omega)} = \frac{\pi\rho}{G(\Omega)}\,. \quad (6.37)$$

In the limit of zero coupling ($J \to 0$) the latter expression yields the SNR (2.16) which is derived for a single element in the framework of the two-state theory [28]:

$$\mathrm{SNR}_0 = \frac{\pi\alpha}{4T^2} = \frac{\pi}{4T^2}\exp\left(-\frac{1}{T}\right). \tag{6.38}$$

The SPA (6.36) as well as the renormalized SNR (6.37) depend on three parameters: (i) the temperature T; (ii) the coupling coefficient J, and (iii) the signal frequency Ω. For a finite value of the signal amplitude A relation (6.32) sets a lower boundary for T and an upper boundary for J. But these restrictions are not principal since in the framework of the weak-field approximation the signal amplitude may be taken to be arbitrarily small.

The dependence of the amplification factor ρ on J and T is shown in Fig. 14. This quantity possesses a single maximum for any time-varying signal as the temperature and the coupling coefficient are varied. The partial derivatives of the SPA taken with respect to the temperature T and the coupling coefficient J vanish for values $(T_{\max}, J_{\max})$ which can be obtained from the transcendent equations

$$J_{\max} = -\frac{T_{\max}}{4}\ln(2T_{\max} - 1), \tag{6.39}$$

$$\Omega^2 = \exp\left(-\frac{2}{T_{\max}}\right)\frac{(2T_{\max} - 1)^2}{T_{\max}(1 - T_{\max})}. \tag{6.40}$$

For a finite and real $J_{\max}$, the condition $T_{\max} > 1/2$ should be valid. In this case Eqn (6.40) has a unique solution $1/2 < T_{\max} < 1$ for any signal frequency $\Omega > 0$. The corresponding $J_{\max}$ may be found from Eqn (6.39). The magnitude of the maximal amplification factor is given as

$$\rho_{\max} = \frac{1 - T_{\max}}{T_{\max}^2(2T_{\max} - 1)}. \tag{6.41}$$

From (6.39), (6.40) and (6.41) we can establish the following properties of the maximum. As the signal frequency Ω varies from very large to vanishingly small values, the optimal temperature $T_{\max}$ falls from 1 to 1/2. In this case the optimal coupling coefficient $J = J_{\max}$ and maximal amplification increase from vanishingly small to very large magnitudes.

We compare the SPA of coupled and uncoupled elements. Let the amplification factor of the uncoupled spin be maximal at a certain temperature T_0 derived from the transcendent equation

$$\Omega^2 = \exp\left(-\frac{2}{T_0}\right)\frac{T_0}{1 - T_0} \tag{6.42}$$

and lie within the interval $0 < T_0 < 1$. The maximal amplification is given as $\rho_0 = (1 - T_0)/T_0^2$. Since $J_{\max}$ is always positive, then for any $\Omega > 0$ the maximal SPA of the coupled element always exceeds the amplification factor of the uncoupled element. In the general case, using (6.40) and (6.42), one may show that $T_{\max}$ is always larger than T_0. However, at relatively high frequencies $\Omega > 1$ the coupling-induced amplification enhancement becomes vanishingly small. Here the amplification maximum is located at $T = T_0$ and $J = 0$.

At low signal frequencies, the amplification is improved by means of ferromagnetic coupling between spins, whereas at high frequencies such an improvement does not exist. The SPA in the low-frequency range qualitatively repeats the effect which was found analytically in Ref. [106] in a system of globally coupled bistable elements. Nevertheless, the amplification behaviour at high frequencies, where with increasing coupling the amplification enhancement is not observed, is a peculiarity of the Glauber model.

The SNR for a single spin demonstrates a similar behaviour. This quantity can be enhanced (compared to the uncoupled chain) via an appropriate coupling between elements [119].

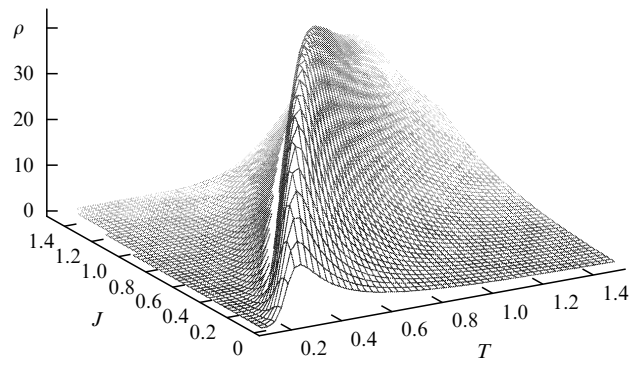

Figure 14. SPA as a function of the temperature T and of the coupling coefficient J. Signal frequency $\Omega = 0.01$.

7. Stochastic synchronization as noise-enhanced order

As has been outlined in Ref. [41], one may associate the switching events with an information flow through a bistable system. Information about the amplitude and the phase of the signal is contained in the times between system's switchings. Indeed, one of the major motivations for SR research is the idea of gaining information transmission through an optimally tuned stochastic bistable filter. The most appropriate measure describing the information transmission through a bistable system is the spectrum of Shannon conditional entropies [120, 121]. In contrast to other measures (a linear version of transinformation) used in Refs [122, 123] and quantifying the degree of linear dependence between the input and the output of the system, the hierarchy of Shannon conditional entropies [124 – 126] characterizes correlations of all higher orders and in the limit is considered to be a measure of the order (disorder) in the system.

The information–theoretical analysis requires the introduction of a symbol alphabet corresponding to the stochastic dynamics of the system. For bistable stochastic systems, a binary alphabet is natural. It consists of two symbols, for instance, '0' and '1', which correspond to the state of the system to the left and to the right with relation to the barrier. Let $\mathbf{i}_n = i_1, \ldots, i_n$ be a binary subsequence of length n or a word of length n (n-word). The stationary probability (estimated from its relative repetition frequency) of such an n-word is denoted by $p(\mathbf{i}_n)$. If a sequence contains a periodic component, then temporal correlations will be reflected by a highly structured n-word distribution function. The residence-time distribution may serve here as its analogue. In order to quantify the degree of order that rules these structures we employ the Shannon entropy [124] which is applied to the n-word distribution

$$H_n = -\sum_{(\mathbf{i}_n)\in\{0,1\}^n} p(\mathbf{i}_n)\log_2 p(\mathbf{i}_n)\,. \tag{7.1}$$

The n-block entropy H_n is interpreted as the average information necessary to predict an appearance of the n-word $(i_1,\ldots,i_n)$.

The conditional or dynamical [125, 126] entropies are introduced for $n = 1, 2, \ldots$ by the following way:

$$h_n = H_{n+1} - H_n = \left\langle -\sum_{i_{n+1}} p(i_{n+1}|\mathbf{i}_n)\log_2 p(i_{n+1}|\mathbf{i}_n)\right\rangle_{(\mathbf{i}_n)}, \tag{7.2}$$

where the angle brackets $\langle\ \rangle$ indicate averaging over the prehistory $\mathbf{i}_n$. This definition is supplemented by 'the initial condition' $h_0 = H_1$. In Eqn (7.2), $p(i_{n+1}|\mathbf{i}_n)$ denotes the appearance probability for the symbol i_{n+1} conditioned by the n preceding symbols $\mathbf{i}_n$. The dynamical entropies h_n are interpreted as the average information necessary to predict the symbol i_{n+1} (or gained after its observation) with given prior knowledge of $\mathbf{i}_n$. In other words, h_n characterizes the uncertainty in prediction of the next symbol in a sequence $\mathbf{i}_n$. This amount of information is usually decreased by correlations between symbols in a sequence. The limit of h_n when $n \to \infty$, i.e.

$$h = \lim_{n\to\infty} h_n\,, \tag{7.3}$$

is named the source entropy [127]. The source entropy determines the minimal amount of information necessary to predict the next symbol in a sequence with given knowledge on the whole prehistory of the process. Only for periodic sequences is this quantity equal to zero. The source entropy is the universal measure of order (disorder) of the system. As is known, the source entropy is connected with the Kolmogorov – Sinaĭ entropy [128, 129].

7.1 Dynamical entropy and source entropy in the regime of stochastic synchronization

We apply the information–theoretical approach to the experimental data obtained for the Schmitt trigger. Binary random sequences generated by a Schmitt trigger were stored in a computer via an analog-digital converter. Simultaneously we recorded the input sequences (the signal and the signal plus noise) which were also represented by 0's and 1's depending on their sign. In all experiments the length of sequences was $15000\Delta t$, where Δt is the step of sampling. The optimal sampling step was chosen to be approximately a twelfth of the signal period: $\Delta t = T_0/12 \approx 8.33\times 10^{-4}$ s. We chose *the regime of synchronization* of stochastic switchings of the trigger when the mean switching frequency is locked. This regime occurs for a signal amplitude $A = 100$ mV.

In order to compare the residence-time distributions at the input and output of the trigger we performed the relevant calculations in the form of histograms. A pronounced peak corresponding to the external signal period is observed at the input only for a small noise intensity. This peak monotonically vanishes with an increase of noise. At the output, on the contrary, there is an optimal noise level at which a similar peak is mostly pronounced. Naturally, the optimal noise intensity corresponds to SR.

It is reasonable to suggest that a symbolic sequence generated by the Schmitt trigger will be maximally ordered in the regime of stochastic synchronization or SR. Hence, one may expect the following scenario for the source entropy behaviour. For very weak noise, when the trigger switching events are very rare, the sequence is characterized by a large redundancy, and the entropy is small. With increasing noise, the entropy should increase and then decrease attaining a minimum due to SR and rise again when the dynamics of the system is fully controlled by noise.

The picture described above was completely verified by the calculations performed from experimental data [120, 121]. All entropy measures were computed by averaging over 20 time series of length $1500\Delta t$. The results are shown in Fig. 15a. The curves in this figure display a well marked minimum around the expected noise intensity. Thus, the predictability of the output sequences can be maximized by tuning the noise intensity! This important effect cannot be principally observed at the output of conventional linear filters.

The increase of predictability implies an enhancement of ordering in the output sequence. With application to stochastic resonance, entropies reflect an amplification of a periodic component of the output signal and for a certain optimal noise level we may speak about *noise-enhanced order* in time. The most ordered state means that a maximal number of switching events takes place during a time equal to the half signal period, and the output is characterized by the longest correlations.

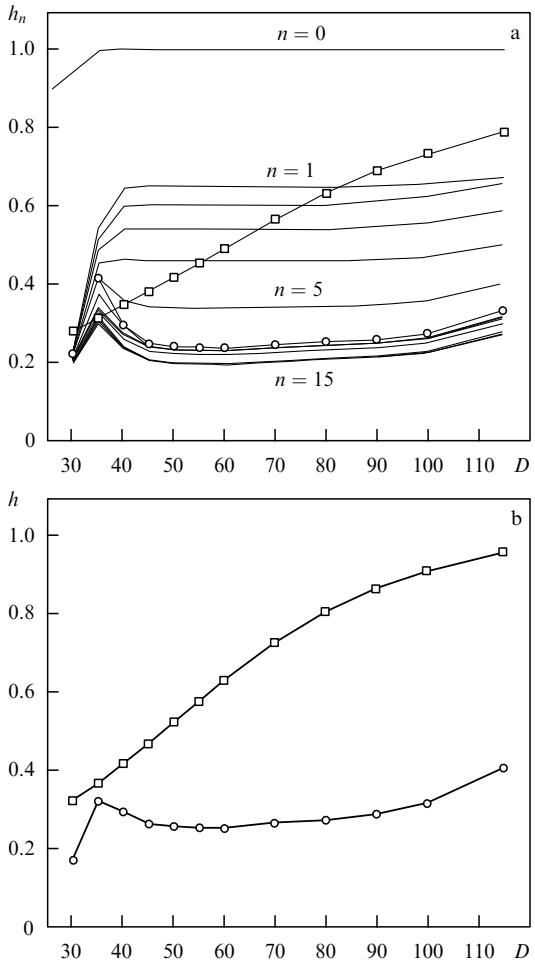

Figure 15. (a) Dynamical entropies h_n $(n = 0, 1, \ldots, 15)$ vs. noise intensity. $h_6(D)$ at the trigger input is shown by the symbols □, $h_6(D)$ at the output is shown by the symbols ○. (b) The source entropy calculated from the residence-time distribution of the trigger over metastable states (symbols ○). The source entropy at the input is shown by the symbols □.

The source entropy h may also be estimated via the residence-time distribution [130]:

$$h = \frac{H[p_{\rm res}]}{\langle t_{\rm res}\rangle}\,, \tag{7.4}$$

where $H[p_{\rm res}]$ denotes the Shannon entropy of the residence-time distribution, and $\langle t_{\rm res}\rangle$ is the mean residence time. In Fig. 15b we plotted the source entropy $h(D)$ calculated from the residence-time distribution as a function of the noise intensity, which is equivalent to the above-considered Shannon conditional (dynamical) entropies: the well-pronounced minimum corresponding to mostly ordered state of the system is observed at the optimal noise intensity. Detailed numerical simulations have shown that the minimum of entropies refers to the SR regime when the output SPA is maximal [120, 121].

Notice that the minimum of the dependence of the source entropy on the noise intensity is observed only for large enough amplitudes of the periodic signal, when the synchronization phenomenon of trigger stochastic switchings occurs. In the case of a weak signal, when the response of a stochastic system to the signal is basically linear, the entropy monotonically grows with increasing noise and tends to 1 in the limit of high noise level [121].

7.2 Stochastic resonance and Kullback entropy

We now turn to the question: when and how do the input and output of a stochastic resonator match? An information–theoretical measure used for this purpose is given by the Kullback entropy $K[p^0, p]$ characterizing the proximity of two distributions p^0 and p [131]:

$$K[p^0, p] = \sum_i p_i \log_2 \frac{p_i}{p_i^0}\,. \tag{7.5}$$

The Kullback entropy determines the amount of information gained by replacing an initial distribution p^0 by a final distribution p due to some transformation. $K[p^0, p]$ is always nonnegative and it vanishes if and only if p^0 and p are identical. For the SR conditions it is natural to identify p^0 with the trigger input distribution $p_i^0 = p_n^{\rm in}(\mathbf{i}_n)$, and p with the output distribution $p_i = p_n^{\rm out}(\mathbf{i}_n)$. Let us consider two cases of the input distribution: firstly, the input distribution is calculated from the signal plus applied noise, and, secondly, the input distribution is calculated from the periodic signal alone.

The calculated Kullback entropy for the first case is shown in Fig. 16a; n ranges from 1 to 8. Common to all curves is a relatively pronounced minimum at $D = 40$ mV, indicating that for this value of the noise intensity the distributions of the input and output match maximally. However, it does not mean that the output sequence maximally reflects the periodic structure. For very weak noise the input sequence is closest to the periodic structure whereas the trigger output sequence is intermittent (long parts are present with identical symbols). Accordingly both distributions are vastly different. With increasing noise intensity towards the SR region the periodic component of the input sequence gets blurred. But now the output signal acquires more and more periodic structure. Hence, both distributions converge at a value of the noise intensity that is less than the resonance one ($D = 60$ mV). We note that the value $D = 40$ mV exactly corresponds to the onset of the synchronization (the mean switching frequency locking) as clearly seen from Fig. 7a.

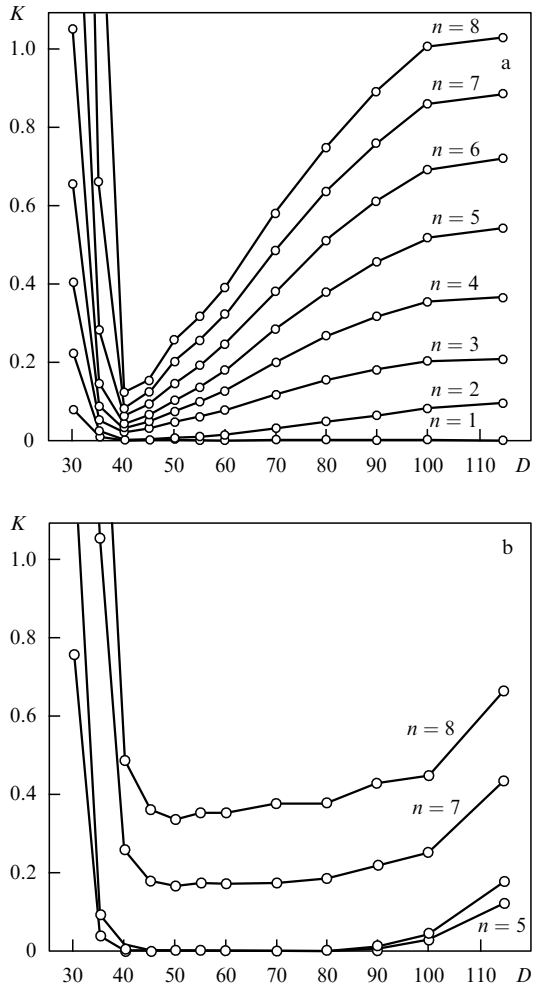

Figure 16. Kullback entropy vs. noise intensity for different word lengths n. (a) The input consists of the signal and noise. (b) The input distribution is given by the signal only.

Figure 16b gives the Kullback entropy for the second case, when the initial distribution is taken from a purely periodic signal. In this case both distributions are closest when the output sequence maximally reflects the periodic structure of the signal and the Kullback entropy takes its minimum in the region of SR at $D = 60$ mV. We note that for $n < 7$ the Kullback entropy equals zero in the region of synchronization because the switchings are synchronized by the signal over time intervals exceeding the half period.

7.3 Enhancement of the degree of order in an ensemble of stochastic oscillators in the SR regime

The fact that the degree of order is enhanced in the regime of SR is also verified when analyzing the collective output of an ensemble of stochastic resonators driven by a weak periodic signal. In order to calculate the source entropy of the collective output of an array we introduce a symbolic description

$$u(t) = \begin{cases} 0, & x_M(t) < 0\,, \\ 1, & x_M(t) \geqslant 0\,. \end{cases} \tag{7.6}$$

The calculated results for the source entropy h are shown in Fig. 17.

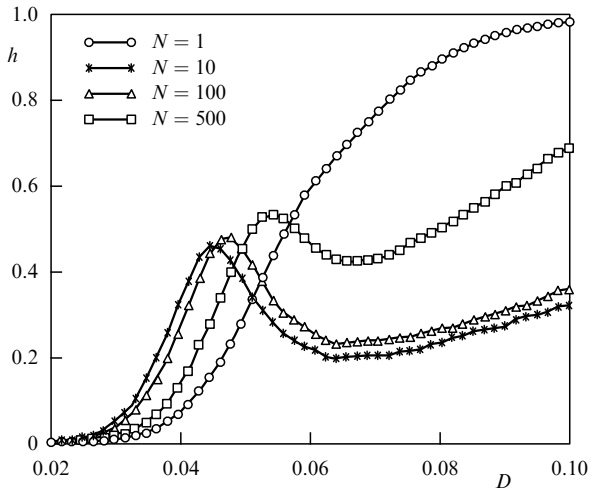

Figure 17. Source entropy of a binary sequence generated by an ensemble of Schmitt triggers vs. internal noise intensity for different numbers of elements in the ensemble.

For a single element, $N = 1$, the entropy monotonically increases with increasing internal noise intensity D and then saturates. When the number of elements goes up, the behaviour of the entropy qualitatively changes. For a weak internal noise, the residence times are exponentially large and the symbolic sequence generated by the array is characterized by high redundancy. As a result, the entropy is close to zero. With increasing D, the source entropy rises and reaches a maximum at the internal noise intensity corresponding to the boundary of the synchronization region, when the mean frequency is locked. Starting from this value the source entropy falls, approaches a minimum at a certain optimal internal noise intensity, and finally rises again. Hence, with increasing internal noise intensity the collective output of the array of stochastic resonators becomes more ordered. We underline that in contrast to the synchronization of a single element by a periodic signal with large amplitude, in the case of an ensemble of stochastic resonators the entropy decreases for weak signals and, hence, single elements remain non-synchronized. Extensive numerical investigations have shown that the values of the noise intensity which minimize the source entropy and the diffusion coefficient are the same as the optimal noise level maximizing the output SPA of a single element.

8. Stochastic resonance and biological information processing

The SR effect is widely used to explain many physical and chemical processes and phenomena as well as for creating a number of technical devices. For example, on the basis of SR one may design an amplifier with a power amplification of the periodic signal attaining $\simeq 30$ dB when the integral power of external noise exceeds the energy of the information-carrying signal by 60 – 70 dB [132]. Under certain conditions, in the presence of high noise level one may supply not only effective amplification, but also extract the signal from the noise when the SNR at the output is significantly larger than the SNR at the input [133].

However, from the point of view of fundamental natural sciences, applications of SR to sensory biology are most interesting and, perhaps, most important. There are several reasons to believe that living organisms have adapted with evolution to use the inevitable internal noise and noisy environment for optimal detection and extraction of useful information. In particular, it has been demonstrated by research of sensory processes in the hydrodynamically sensitive mechanoreceptors of the crayfish [134, 135] and the air motion-sensitive receptors of the cricket [123]. These sensory systems in both animals were presumably evolved for the purpose of long-range detection of predators: in the case of the crayfish — a hungry fish, and in the case of the cricket — a wasp, which seeks to lay eggs within the body of the animal. For successful predator avoidance crayfishes are adept at detecting well in advance the nearly periodic signal of the water vibrations generated by the tail of a swimming predator fish on the background of water turbulence, and crickets — the periodic air vibrations due to the wing beats of wasps on the background of a noisy environment. As has been shown, the theory of non-dynamical or threshold SR is capable of explaining the sensory mechanisms of these animals. What is more, this theory makes possible a qualitative explanation of the peculiarities of human visual perception [136, 137].

8.1 Stochastic resonance in the mechanoreceptors of the crayfish

The mechanoreceptor system of the crayfish is located in its tailfan and is illustrated in Fig. 18. The tailfan has approximately 250 long hairs which are connected to the interneurons within the ganglion by sensory neurons collected into nine nerve roots.

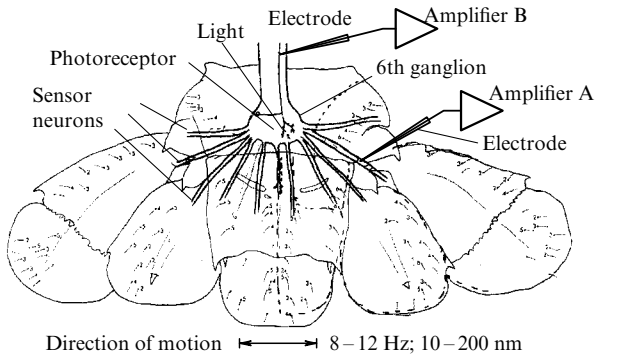

Figure 18. Mechanoreceptor system of the crayfish.

The tailfan has the 6th, or terminal, ganglion with its pair of photoreceptor cells. As seen from Fig. 18, neural impulses can be registered at the sensory neurons, or on the photoreceptor output neuron. In order to record the neuron signals, the microelectrodes were surgically introduced into desired parts of the crayfish receptor system. The hairs were stimulated by relative fluid motions in the directions shown in Fig. 18. These motions are typically sinusoidal, of amplitude 10 to 100 nanometers, at frequencies from 5 to 100 Hz, and velocities 100 to 1000 microns per second. The responses of a photoreceptor cell can be studied in the presence of both hydrodynamical stimulation and light beam of uniform intensity on the photoreceptive area. Environmental noise was used as the random source. The experimental protocols necessary for this research have been well-developed [134].

Measurements of the SNR of the crayfish sensory neuron as a function of the external noise intensity have demonstrated the effect of SR. The experimental results are shown by the squares in Fig. 19, where the theory is exhibited by the solid curve and a FitzHugh – Nagumo simulation is depicted by the diamonds. These results suggest that the mechanoreceptor system provides signal detection in environmental noise of an optimal intensity. Moreover, the signals best detected are sinusoidal in the frequency range around 10 Hz. This is the frequency characteristic of water vibrations induced by swimming fish. Such water waves travel faster than the fish itself thus providing an early warning of the crayfish.

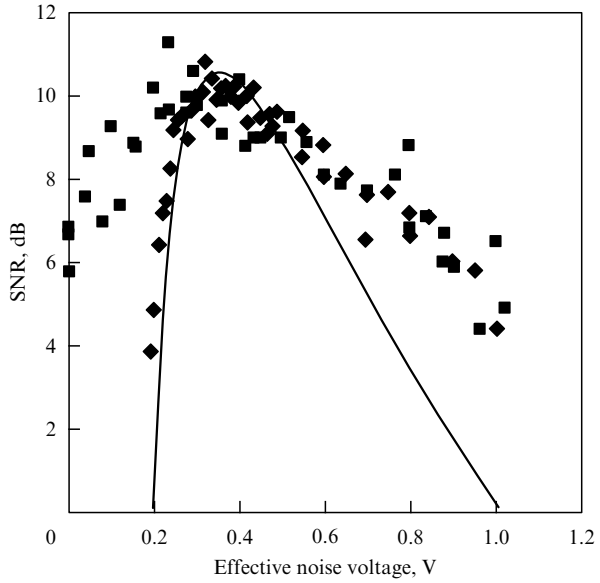

Figure 19. Crayfish sensory SR is illustrated by the squares, compared to the theory (solid line) and FitzHugh – Nagumo simulation (◆).

A major question concerning the internal noise of sensory (and other) neurons remains open. Virtually all neurons are noisy [138, 139], and some are much more noisier than can be accounted for by equilibrium statistical processes [140]. Experiments designed to seek SR in the crayfish sensory neurons have been performed by controlling the internal noise through the variation of temperature of the preparation. Unfortunately, SR has not been observed yet.

8.2 The photoreceptor system of the crayfish

There is another way to control the internal noise of a neuron, which has resulted in observation of SR. The light falling on a photoreceptive area embedded in the 6th ganglion mediates the internal noise of that neuron (see Fig. 18) [135]. Our current state of knowledge of the detailed mechanism of the interplay between light intensity and the level of neuron internal noise is far from satisfactory. The neural output at this location is determined by the complex (and largely not understood) computational processes occurring within the ganglion. However, recordings from the photoreceptor output neuron as the light intensity is varied have shown that an increase of the light intensity causes the internal noises to grow. This fact suggests the possibility of studying the influence of the internal noise of a neuron on its ability for periodic signal detection. In the experiments, hydrodynamic stimuli were applied to the crayfish receptors as usual, but the signal-to-noise ratio was measured for different light intensities. The experimental data surely confirmed the SR effect controlled by light intensity.

The experimental results outlined above have been confirmed in a recent experiment on SR with crickets [123]. The crickets make use of a similar wasp avoidance system. The cricket has two rear appendages which are covered with hair mechanoreceptors. Each receptor is connected to a set of interneurons in a terminal ganglion very much like that of the crayfish. The hairs respond to air vibrations and have characteristic frequencies of 80 to 150 Hz. (By contrast, the crayfish mechanoreceptive system responds to hydrodynamic stimuli of 8 to 25 Hz.) The wing beats of the wasp, the main predator of the cricket, lie within this frequency range.

The SR experiment on the cricket was designed with many improvements. For example, modern information transmission measures rather than the simple SNR measure were used. A weak periodic stimulus was applied to the appendages in the form of air flows to which random motions (noise) were added. The results showed an optimal external noise intensity for which the transinformation from stimulus to interneurons in the ganglion was maximum. Moreover, the results brought out that the addition of external noise to a weak periodic signal could also improve the neural-action potential timing precision.

8.3 SR as a tool for quantifying human visual processes

Practically in all the experiments on studying SR effect, the computer analysis of signals at the input and output of the systems under consideration was employed, which lent support to the conclusion about a presence of signal amplification (or information gain) under the action of intensity-optimal noise. But does the animal or a human actually make use of this enhanced information? That cannot be shown by any direct electrophysiological recording, but instead must be tested integrally in behavioural, that is psychological, experiments in humans. The original motivation of such experiments was to replace the complex computer-assisted data analysis with a human perception (interpretation). Thus psychophysics experiments were designed to explore the human ability to interpret noise-enhanced visual information. Will this visually perceived information depend on the noise intensity in a nonlinear way similar to the SR effect? Is it possible to introduce any quantitative criterion for the optimal interpretation of visual information? These questions were answered in Ref. [137]. The answer is positive.

The experiments have been described in detail elsewhere [137] and so will only briefly be outlined here. A picture was digitized on a 256 level gray scale and displayed on a computer monitor as an image of 256 by 256 pixels. The picture was then sunk beneath a threshold. The gray values of all pixels lie beneath the threshold so the image on the monitor is blank. Noise is then added to this threshold image by choosing a number from a zero-mean Gaussian distribution and adding this to the image pixel-by-pixel. The noise in each pixel is uncorrelated with the noise in any other pixel. Some pixels now contain gray levels above the threshold, and these are shown completely black. The remaining pixels (with gray levels below the threshold) are shown white. If the noise added is too small, only a few pixels contain information about the image and the resulting picture is difficult to interpret. If the noise is too large, there is overly

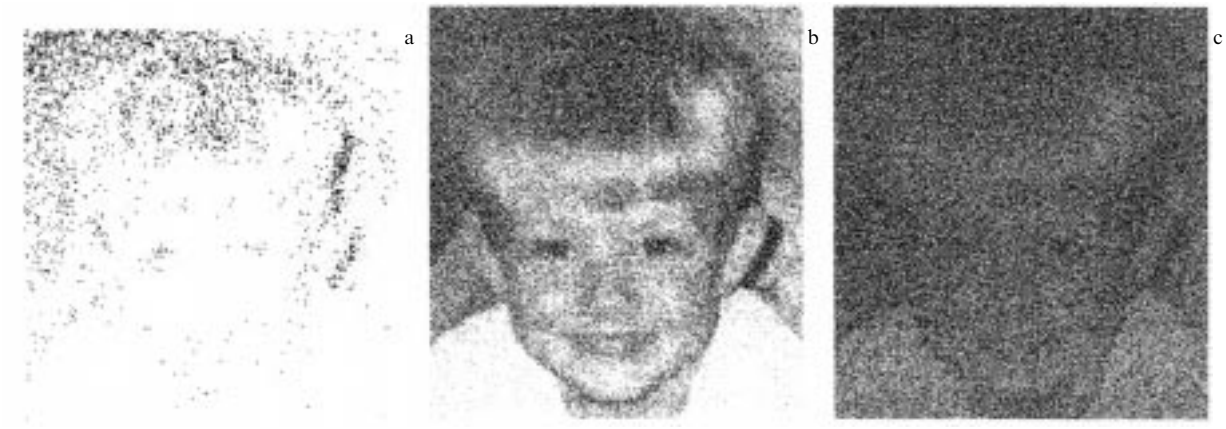

Figure 20. Three pictures of a boy at different noise intensities added to the subthreshold image.

much randomness in the picture and it is again difficult to interpret. An optimal noise level results in the mostly interpretable picture. An example is shown in Fig. 20. Note that one can see the picture very well in Fig. 20b, which shows the optimal noise added. The effects on the human visual system are dynamical, and an interactive animation may be seen on the World Wide Web (http://neurodyn.umsl.edu/sr). In the dynamical presentation, the noise correlation time also has an effect which can be observed at the Web site.

In the psychophysical experiment, subjects were presented with a series of pictures contaminated with noise of varying intensity and/or correlation time. The image used was a standard pattern used in visual psychophysics experiments. Subjects were asked to identify the fine (pleasant) detail of the pattern. Their perceptive threshold A_{th} was measured.

Example data of the perceptive threshold as a function of the noise level for one subject are shown in Fig. 21. Notice that the perceptive threshold registered by the subject is minimum when the information transmitted by the picture to the visual cortex is maximum. Thus the characteristic feature of SR appears in this experiment as a minimum in the perceptive threshold. This fact can be substantiated on the basis of the approximate theory of threshold SR. The standard equation (4.8) describing SR is rewritten as a signal amplitude equation and solved for a multiplicative constant A_{th}, which has the dimension of signal power. All coefficients are lumped into single constant K, which is used as the only adjustable parameter in fitting the psychophysical data with the theory. The equation for A_{th} is shown in legend to Fig. 21 together with the dependence $A_{\text{th}}(\sigma)$ and experimental data in the figure itself. Note that the fit is not excellent, but is surprisingly good in view of the implicit assumptions. In particular, Eqn (4.8) was derived for a single stochastic resonator. But brain processes are rather complex, so there is no reason to suppose that a single-element equation would describe the experimental findings.

Notice that the fitting constant K applies to a single individual subject and is a measure of his or her ability to detect and interpret fine details in a noise-contaminated visual picture. This ability varies considerably from subject-to-subject. However, the dependence presented in Fig. 21 holds for all subjects. What is important, the constant K for different subjects does not change in time. Each subject was tested three times in three sessions separated by at least one day and often as much as a week. The repeatability for an individual subject over the three sessions is worth noting. Moreover, three of the subjects were recalled after approximately a year. Within the limits of experimental accuracy 10–15% the values of K were unvaried. The findings indicate that the experiment produces robust and repeatable results.

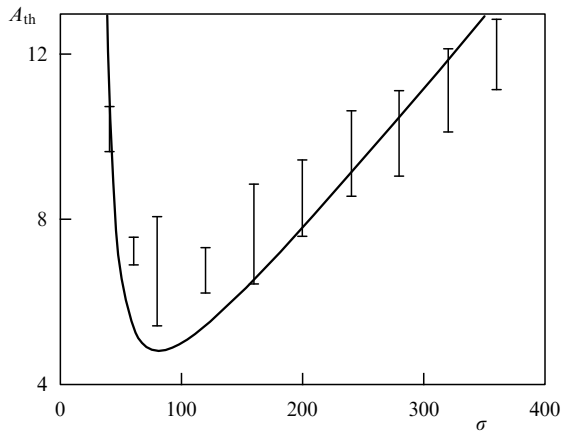

Figure 21. Example of data on perceptive threshold $A_{\text{th}} = K_1 \sigma \exp[\Delta^2/(2\sigma^2)]$ versus effective noise intensity σ; $K = 0.36$ and $\Delta = 81$.

9. Conclusions

In the framework of this review we have analyzed nonlinear phenomena over a wide class of bistable systems simultaneously driven by information-carrying signals of different structures and internal or external noise of a given statistics. All the cases considered here have confidently shown that noise of an optimal intensity can be used to improve certain characteristics of the signal at the output of a bistable system. This phenomenon is known as stochastic resonance. The noise plays a constructive role and can be beneficial to increase different coherence measures as well as the degree of order in the system. From this point of view, SR can be treated as a noise-induced transition, when the degree of order in the system is enhanced due to noise.

Let us summarize briefly the major results of this work. As was shown in Section 3, SR can be used to amplify signals with amplitude and frequency modulation of low-frequency carrier signals on a background of noise of relatively high

intensity. Distortions of the signal cannot be avoided, but they can be minimized by choosing optimal noise and tuning operating characteristics of the system. When a narrow-band (quasi-monochromatic) noisy signal with a finite spectral linewidth is used, then it is possible to minimize the effective width of the spectral line of the output signal. SR is also realized for information-carrying signals with a wide continuous frequency spectrum. A quantitative measure of the degree of order here is the coherence function attaining its maximum when SR occurs. The extension of the SR theory to non-dynamical (or threshold) systems (4.1) is of great interest. The theory of threshold SR is able to describe the active processes in neuron systems and to explain the results of a series of interesting biological experiments (Section 8).

The results on SR in chaotic systems (4.2) are interesting as well. Noise-induced switchings between two chaotic attractors are in agreement with the general conception of the physical mechanism of SR. In contrast to the simple bistable oscillator, here we have 'an interaction' of two metastable states with complex intrawell dynamics. If a two-state approach taking into account only the switching events is applied, then we observe no significant differences. SR observed in the regime of dynamical intermittency (in the absence of noise) is a principally new phenomenon. In this case the effective Kramers time is determined by the system parameter and the SR regime takes place at an optimal value of the control parameter at which the mean switching frequency matches the driving frequency.

One of the basic problems of the review was a detailed analysis of the new phenomenon, i.e. stochastic synchronization of bistable systems (Section 5). Many researchers have indicated in their papers that SR is conditioned by synchronization. But this point was not wholly clear [93]. In this review we have given a clear definition of effective stochastic synchronization, presented a theory of this effect based on the classical works on synchronization of autooscillations in the presence of noise, and presented the results of full-scale and numerical experiments, which completely confirm the theoretical conclusions. Now we can confidently conclude that for finite force amplitudes the effect of instantaneous phase and switching frequency locking takes place over a finite range of system parameter values (in the synchronization region). As a result, there is a range of noise intensities (or another control parameter) where the mean switching frequency is nearly constant and equal to the modulation frequency. As is known, synchronization is one of the possible mechanisms of self-organization in nonlinear systems. The extension of the definition of effective synchronization to a wide class of bistable stochastic systems allows one to understand more clearly the physical mechanism of enhancement of order in noisy bistable systems. As was shown in Section 7, only in the regime of stochastic synchronization do the dynamical entropy and the source entropy reach their minima, indicating an enhancement of order or self-organization in the system.

In Section 6 we studied SR in ensembles of stochastic resonators. We considered ensembles of noninteracting elements, of nondynamical elements and ensembles of coupled elements. We showed that the SR effect can be significantly enhanced in an array compared to a single bistable element. The SNR at the ensemble output in the regime of SR can be close to the SNR at the input with a large amplification factor of the input signal. The array of stochastic resonators, in contrast to a single bistable element, demonstrates the effect of stochastic synchronization for an arbitrarily weak external periodic signal. In addition, the dependence of coherence function on frequency disappears with increasing number of elements in the ensemble. We applied the linear response theory and showed explicitly the effect of SR without tuning: in order to observe SR in a large array one needs only the presence of noise of any intensity. This conclusion is very important since it explains the mechanism of 'noise tuning' in systems of sensory neurons.

Finally, in Section 8 we discussed the results of applications of the SR theory to a possible explanation of the ability of living organisms to detect weak signals in a noisy enough environment. We showed certainly that in the regime of SR some living organisms detect a weak informational signal most efficiently.

The authors would like to thank W Ebeling, J Kurths, P V E McClintock, M I Dykman, P Jung, P Hänggi, J J Collins, S M Soskin, F Marchesoni, and S Bezrukov for the opportunity to discuss the results of this work at numerous special conferences and seminars on nonlinear dynamics. The authors are grateful to E Simonotto, A Pikovsky, M Rozenblyum, Yu Klimontovich, B Shul'gin, I Khovanov, A Sil'chenko, U Siewert, and J Freund for fruitful discussions and valuable remarks, encouraging the improvement of this work, and for the help in performing a series of numerical experiments.

We are delighted to note that all the research reported here was supported by the Russian State Committee of Higher Education (Grants 93-8.2-10, 95-0-8.3-66, 97-0-8.3-47), by the Soros Foundation (Grants RNO 000, RNO 300), by a grant of the Russian Foundation for Basic Research (98-02-16531), by a grant of the U.S. Office of Naval Research, Physics Division, by the common research project of RFBR and DFG (Germany) (Grant 436 RUS 113/334/0(R)), by an INTAS Grant 96-0305, and by a grant of the Royal Society of the UK. A N is a recipient of a Fetzer Institute (USA) postdoctoral fellowship.

The authors are especially grateful to Dr. G Strelkova for her great help in translation and preparation of the manuscript for publication.

References

1. Stratonovich R L *Izbrannye Voprosy Teorii Flyuktuatsiĭ v Radiotekhnike* (Selected Problems of Fluctuation Theory in Radiotechnics) (Moscow: Sov. Radio, 1961)
2. Rytov S M *Vvedenie v Statisticheskuyu Radiofiziku*. T. 1 *Sluchaĭnye Protsessy* (An Introduction to Statistical Radiophysics. Vol. 1 Stochastic Processes) (Moscow: Nauka, 1976) [Translated into English: Rytov S M, Kravtsov Yu A, Tatarskiĭ V I *Principles of Statistical Radiophysics* Vols 1, 2 (Berlin: Springer-Verlag, 1987)]
3. Malakhov A N *Fluktuatsii v Avtokolebatel'nykh Sistemakh* (Fluctuations in Autooscillating Systems) (Moscow: Nauka, 1968)
4. Pontryagin L S, Andronov A A, Vitt A A *Zh. Eksp. Teor. Fiz.* **3** 165 (1933)
5. Landa P S, Zaikin A A *Zh. Eksp. Teor. Fiz.* **111** 358 (1997) [*JETP* **84** 197 (1997)]
6. Horsthemke W, Lefever R *Noise-Induced Transitions* (Springer Series in Synergetics, Vol. 15) (Berlin: Springer-Verlag, 1984) [Translated into Russian (Moscow: Mir, 1987)]
7. Benzi R, Sutera A, Vulpiani A *J. Phys. A* **14** L453 (1981)
8. Benzi R et al. *Tellus* **34** 10 (1982)
9. Nicolis C *Tellus* **34** 1 (1982)
10. Fauve S, Heslot F *Phys. Lett. A* **97** 5 (1983)
11. McNamara B, Wiesenfeld K, Roy R *Phys. Rev. Lett.* **60** 2626 (1988)
12. Grigorenko A N et al. *J. Appl. Phys.* **76** 6335 (1994)

13. Dykman M I et al. *Pis'ma Zh. Eksp. Teor. Fiz.* **53** 182 (1991) [*JETP Lett.* **53** 193 (1991)]
14. Gammaitoni L et al. *Phys. Rev. Lett.* **67** 1799 (1991)
15. Simon A, Libchaber A *Phys. Rev. Lett.* **68** 3375 (1992)
16. Spano M L, Wun-Fogle M, Ditto W L *Phys. Rev. A* **46** R5253 (1992)
17. Mantegna R N, Spagnolo B *Phys. Rev. E* **49** R1792 (1994)
18. Hibbs A D et al. *Nuovo Cimento* **17D** 811 (1995)
19. Perez-Madrid A, Rubi J M *Phys. Rev. E* **51** 4159 (1995)
20. Neda Z *Phys. Lett. A* **210** 125 (1996)
21. Dubinov A E et al. *Izv. Ross. Akad. Nauk Ser. Fiz.* **60** (10) 76 (1996)
22. Leonard D S, Reichl L E *Phys. Rev. E* **49** 1734 (1994)
23. Dykman M I, Horita T, Ross J *J. Chem. Phys.* **103** 966 (1995)
24. Hohmann W, Muller J, Schneider F W *J. Phys. Chem.* **100** 5388 (1996)
25. Babinec P *Phys. Lett. A* **225** 179 (1997)
26. Kramers H A *Physica* **7** 284 (1940)
27. Hänggi P, Talkner P, Borkovec M *Rev. Mod. Phys.* **62** 251 (1990)
28. McNamara B, Wiesenfeld K *Phys. Rev. A* **39** 4854 (1989)
29. Zhou T, Moss F, Jung P *Phys. Rev. A* **42** 3161 (1990)
30. Gammaitoni L et al. *Phys. Rev. Lett.* **62** 349 (1989)
31. Gammaitoni L, Marchesoni F, Santucci S *Phys. Rev. Lett.* **74** 1052 (1995)
32. Fox R F *Phys. Rev. A* **39** 4148 (1989)
33. Stocks N G, Stein N D, McClintock P V E *J. Phys. A* **26** L385 (1993)
34. Anishchenko V S, Neiman A B, Safonova M A *J. Stat. Phys.* **70** (1 – 2) 183 (1993)
35. Anishchenko V S, Safonova M A, Chua L O *Int. J. Bif. Chaos* **2** 397 (1992)
36. Gingl Z, Kiss L B, Moss F *Europhys. Lett.* **29** 191 (1995)
37. Jung P *Phys. Rev. E* **50** 2513 (1994); *Phys. Lett. A* **207** 93 (1995)
38. Neiman A, Schimansky-Geier L *Phys. Rev. Lett.* **72** 2988 (1994)
39. Hänggi P et al. *J. Stat. Phys.* **70** (1 – 2) 25 (1993)
40. Neiman A, Sung W *Phys. Lett. A* **224** 341 (1996)
41. Moss F, in *Some Problems in Statistical Physics* (Philadelphia: SIAM, 1994) p. 205
42. Moss F, Pierson D, O'Gorman D *Int. J. Bif. Chaos* **4** 1383 (1994)
43. Bulsara A R, Gammaitoni L *Phys. Today* **49** (3) 39 (1996)
44. Gammaitoni L et al. *Rev. Mod. Phys.* **70** 223 (1998)
45. Proc. NATO Adv. Res. Workshop on Stochastic Resonance in Physics and Biology *J. Stat. Phys.* **70** (1 – 2) (1993)
46. Proc. Int. Workshop on Fluctuations in Physics and Biology: Stochastic Resonance, Signal Processing and Related Phenomena *Nuovo Cimento* **17D** (7 – 8) (1995)
47. Gammaitoni L, WWW Internet server: http://www/pg.infnit/SR/index.html
48. Gardiner C V *Handbook of Stochastic Methods for Physics, Chemistry, and the Natural Sciences* (Springer Series in Synergetics, Vol. 13) (Berlin: Springer-Verlag, 1983) [Translated into Russian (Moscow: Mir, 1986)]
49. Jung P, Hänggi P *Phys. Rev. A* **41** 2977 (1990)
50. Jung P, Hänggi P *Phys. Rev. A* **44** 8032 (1991)
51. Jung P *Phys. Rep.* **234** 175 (1993)
52. Landau L D, Lifshitz E M *Statisticheskaya Fizika* Chast' 1 (Statistical Physics. Part 1) (Moscow: Nauka, 1976) [Translated into English (Oxford: Pergamon Press, 1980)]
53. Balescu R *Equilibrium and Nonequilibrium Statistical Mechanics* (New York: Wiley, 1975) [Translated into Russian (Moscow: Mir, 1978)]
54. Hänggi P, Thomas H *Phys. Rep.* **88** 207 (1982)
55. Dykman M I et al. *Pis'ma Zh. Eksp. Teor. Fiz.* **52** 780 (1990) [*JETP Lett.* **52** 141 (1990)]
56. Dykman M I et al. *Phys. Lett. A* **180** 332 (1993)
57. Dykman M I et al. *Phys. Rev. Lett.* **68** 2985 (1992)
58. Kubo R *J. Phys. Soc. Jpn.* **12** 570 (1957); *Rep. Prog. Phys.* **29** 255 (1966)
59. Risken H *The Fokker – Planck Equation* 2nd ed. (Springer Series in Synergetics, Vol. 18) (Berlin: Springer-Verlag, 1989)
60. Anishchenko V S et al. *Radiotekh. Elektron.* **39** 1380 (1994)
61. Anishchenko V S et al., in *Chaos and Nonlinear Mechanics: Proceedings Euromech Colloquium* (Eds T Kapitaniak, J Brindley) (Singapore: World Scientific, 1995) p. 41
62. Anishchenko V S, Safonova M A, Chua L O *Int. J. Bif. Chaos* **4** 441 (1994)
63. Klimontovich Yu L *Statisticheskaya Fizika* (Statistical Physics) (Moscow: Nauka, 1982) [Translated into English (Chur: Harwood Acad. Publ., 1986)]
64. Schimansky-Geier L, Zülicke Ch *Z. Phys. B* **79** 451 (1990)
65. Collins J J, Chow C C, Imhoff T T *Phys. Rev. E* **52** R3321 (1995)
66. Collins J J, Chow C C, Imhoff T T *Phys. Rev. E* **54** 5575 (1996)
67. Chialvo, Longtin A, Müller-Gerking J *Phys. Rev. E* **55** 1798 (1997)
68. Neiman A, Schimansky-Geier L, Moss F *Phys. Rev. E* **57** R9 (1997)
69. Dykman M I et al. *Nuovo Cimento* **17D** 661 (1995)
70. Rice S O, in *Selected Papers on Noise and Stochastic Processes* (Ed. N Wax) (New York: Dover, 1954) p. 133
71. Anishchenko V S *Slozhnye Kolebaniya v Prostykh Sistemakh* (Complex Oscillations in Simple Systems) (Moscow: Nauka, 1990)
72. Kifer Yu I *Izv. Akad. Nauk SSSR Ser. Math.* **38** 1091 (1974)
73. Kifer Yu *Commun. Math. Phys.* **121** 445 (1989)
74. Vul E B, Sinaĭ Ya G, Khanin K M *Usp. Mat. Nauk* **39** (3) 3 (1984)
75. Anishchenko V S, Ebeling W *Z. Phys. B* **81** 445 (1990)
76. Ventzel' A D, Freĭdlin M I *Fluktuatsii v Dinamicheskikh Sistemakh pod Deĭstviem Malykh Sluchaĭnykh Vozmushchenii* (Fluctuations in Dynamical Systems under Influence of Random Perturbations) (Moscow: Nauka, 1979) [Translated into English: Freidin M I, Wentzell A D *Random Perturbations of Dynamical Systems* (Grundlehren der mathematischen wissenschaften, 260) (New York: Springer-Verlag, 1984)]
77. Graham R, in *Noise in Nonlinear Dynamical Systems* Vol. 1 *Theory of Continuous Fokker – Planck Systems* (Eds F Moss, P V E McClintock) (Cambridge: Cambridge University Press, 1988)
78. Graham R, Hamm A, Tel T *Phys. Rev. Lett.* **66** 3089 (1991)
79. Klimontovich Yu L *Turbulentnoe Dvizhenie i Struktura Khaosa* (Turbulent Motion and the Structure of Chaos) (Moscow: Nauka, 1990) [Translated into English (Dordrecht: Kluwer Acad. Publ., 1991)]
80. Anishchenko V S *Pis'ma Zh. Tekh. Fiz.* **10** 629 (1984) [*Sov. Tech. Phys. Lett.* **10** 266 (1984)]
81. Anishchenko V S, Neiman A B *Pis'ma Zh. Tekh. Fiz.* **17** 1063 (1987) [*Sov. Tech. Phys. Lett.* **13** 444 (1987)]
82. Anishchenko V S, Neiman A B *Zh. Tekh. Fiz.* **60** (1) 3 (1990) [*Sov. Phys. Tech. Phys.* **35** 1 (1990)]
83. Anishchenko V S, Neiman A B, Chua L O *Int. J. Bif. Chaos* **4** 99 (1994)
84. Lorenz E N *J. Atmos. Sci.* **20** 130 (1963)
85. Klimontovich Yu L (Ed.) *Volnovye i Fluktuatsionnye Protsessy v Lazerakh* (Wave and Fluctuation Processes in Lasers) (Moscow: Nauka, 1974)
86. Ito H M *J. Stat. Phys.* **35** 151 (1984)
87. Bykov V V, Shil'nikov A L, in *Metody Kachestvennoĭ Teorii i Teorii Bifurkatsiĭ* (Methods of the Qualitative Theory and the Theory of Bifurcations) (Gor'kiĭ: GGU, 1989) p. 151
88. Anishchenko V S, Neiman A B *Pis'ma Zh. Tekh. Fiz.* **17** 43 (1991) [*Sov. Tech. Phys. Lett.* **17** 510 (1991)])
89. Rabinovich M I *Usp. Fiz. Nauk* **125** 123 (1978) [*Sov. Phys. Usp.* **21** 443 (1978)]
90. Shulgin B, Neiman A, Anishchenko V *Phys. Rev. Lett.* **75** 4157 (1995)
91. Anishchenko V, Neiman A, in *Stochastic Dynamics* (Lecture Notes in Physics, Vol. 484, Eds L Schimansky-Geier, T Pöschel) (Berlin: Springer-Verlag, 1997) p. 155
92. Anishchenko V S, Neiman A B *Izv. Vyssh. Uchebn. Zaved. Prikladnaya Nelineĭnaya Dinamika* **5** (1) 5 (1997)
93. Neiman A et al. *Phys. Rev. E* **58** (6) (1998)
94. Neiman A *Phys. Rev. E* **49** 3484 (1994)
95. Gabor D *J. IEE* (London) **93** 429 (1946); Panter P F *Modulation, Noise and Spectral Analysis, Applied to Information Transmission* (New York: McGraw-Hill, 1965)
96. Vaĭnshteĭn L A, Vakman D E *Razdelenie Chastot v Teorii Kolebaniĭ i Voln* (Frequency Separation in the Theory of Oscillations and Waves) (Moscow: Nauka, 1983)
97. Middleton D *An Introduction to Statistical Communication Theory* (New York: McGraw-Hill, 1960)
98. Levin B R *Teoreticheskie Osnovy Radiotekhniki* Kniga 1 (Theoretical Foundations of Radio Engineering, Vol. 1) (Moscow: Sov. Radio, 1974)
99. Rosenblum M, Pikovsky A, Kurths J *Phys. Rev. Lett.* **76** 1804 (1996)

100. Shalfeev V, in *Sistemy Fazovoĭ Sinkhronizatsii* (Systems with Phase Synchronization) (Eds V V Shakhgil'dyan, L N Belyustina) (Moscow: Radio i Svyaz', 1982) p. 95
101. Neiman A, Feudel U, Kurths J *J. Phys. A: Math. Gen.* **28** 2471 (1995)
102. Melnikov V I *Phys. Rev. E* **48** 2481 (1993)
103. Neiman A, Schimansky-Geier L *Phys. Lett. A* **197** 379 (1995)
104. Anishchenko V S, Silchenko A N, Khovanov I A *Phys. Rev. E* **57** 316 (1997)
105. Bulsara A, Schmera G *Phys. Rev. E* **47** 3734 (1993)
106. Jung P et al. *Phys. Rev. A* **46** R1709 (1992)
107. Inchiosa M E, Bulsara A R *Phys. Rev. E* **52** 327 (1995)
108. Linder J F et al. *Phys. Rev. Lett.* **75** 3 (1995)
109. Schimansky-Geier L, Siewert U, in *Stochastic Dynamics* (Eds L Schimansky-Geier, T Pöschel) (Berlin: Springer-Verlag, 1997) p. 245
110. Bendat J S, Piersol A G *Random Data. Analysis and Measurement Procedures* (New York: John Wiley & Sons, 1986) [Translated into Russian (Moscow: Mir, 1989)]
111. Pei X, Wilkens L, Moss F *Phys. Rev. Lett.* **77** 4679 (1996)
112. Bezrukov S M, Vodyanoy I *Nature* (London) **378** 362 (1995)
113. Gailey P C et al. *Phys. Rev. Lett.* **79** 4701 (1997)
114. Pikovskiĭ A S *Izv. Vyssh. Uchebn. Zaved. Ser. Radiofiz.* **27** 576 (1984)
115. Collins J J, Chow C C, Imhoff T T *Nature* (London) **376** 236 (1995)
116. Neiman A, Moss F, Schimansky-Geier L, Ebeling W, in *Applied Nonlinear Dynamics and Stochastic Systems Near the Millenium* (AIP Conf. Proc., Vol. 411, Eds J B Kadtke, A R Bulsara) (New York: AIP, 1997) p. 151
117. Glauber R J *J. Math. Phys.* **4** 294 (1963)
118. Brey J J, Prados A *Phys. Lett. A* **216** 240 (1996)
119. Siewert U, Schimansky-Geier L *Phys. Rev. E* **58** 2843 (1998)
120. Neiman A et al. *Phys. Rev. Lett.* **76** 4299 (1996)
121. Schimansky-Geier L et al. *Int. J. Bif. Chaos* **8** 869 (1998)
122. Bulsara A, Zador A *Phys. Rev. E* **54** R2185 (1996)
123. Levin J E, Miller J P *Nature* (London) **380** 165 (1996)
124. Shannon C E *Raboty po Teorii Informatsii i Kibernetike* (Works on Information Theory and Cybernetics) (Moscow: IL, 1963) [see: *Claude Elwood Shannon*: *Collected Papers* (Eds W J A Sloane, A D Wyner) (New York: IEEE Press, 1993)]
125. Ebeling W, Nicolis G *Chaos, Solitons and Fractals* **2** 635 (1992)
126. Ebeling W, Freund J, Rateitschak K *Int. J. Bif. Chaos* **6** 611 (1996)
127. Khinchin A Ya *Usp. Mat. Nauk* **11** (1) 17 (1956)
128. Eckmann J-P, Ruelle D *Rev. Mod. Phys.* **57** 617 (1985)
129. Pesin Ya B *Usp. Mat. Nauk* **32** (4) 55 (1977)
130. Freund J *Phys. Rev. E* **53** 5793 (1996)
131. Kullback S *Information Theory and Statistics* (New York: John Wiley & Sons, 1959) [Translated into Russian (Moscow: Nauka, 1967)]
132. Shul'gin B V *Thesis for Candidate of Physicomathematical Sciences* (Saratov: Saratov State University, 1996)
133. Khovanov I A, Anishchenko V S, in *Applied Nonlinear Dynamics and Stochastic Systems Near the Millenium* (AIP Conf. Proc., Vol. 411, Eds J B Kadtke, A R Bulsara) (New York: AIP, 1997) p. 267
134. Douglass J K et al. *Nature* (London) **365** 337 (1993)
135. Pei X, Wilkens L, Moss F *J. Neurophysiol.* **76** 3002 (1996)
136. Riani M, Simonotto E *Phys. Rev. Lett.* **72** 3120 (1994)
137. Simonotto E et al. *Phys. Rev. Lett.* **78** 1186 (1997)
138. Moore G, Perkel D, Segundo J *Ann. Rev. Physiol.* **28** 493 (1966)
139. Adey W R *Int. J. Neurosci.* **3** 271 (1972)
140. Denk W, Webb W *Hears. Res.* **60** 89 (1992)